Bioorganic & Medicinal Chemistry 18 (2010) 3518–3534

Contents lists available at ScienceDirect

Bioorganic & Medicinal Chemistry

journal homepage: www.elsevier.com/locate/bmc

Virtual screening, selection and development of a benzindolone structural scaffold for inhibition of lumazine synthase

Arindam Talukdar [a], Ekaterina Morgunova [b], Jianxin Duan [d], Winfried Meining [e], Nicolas Foloppe [b], Lennart Nilsson [b], Adelbert Bacher [c], Boris Illarionov [c], Markus Fischer [c], Rudolf Ladenstein [b], Mark Cushman [a,*]

[a] Department of Medicinal Chemistry and Molecular Pharmacology, School of Pharmacy and Pharmaceutical Sciences, and The Purdue Center for Cancer Research, Purdue University, West Lafayette, IN 47907, USA
[b] Karolinska Institute, Department of Bioscience, Hälsovägen 7-9, S-14157 Huddinge, Sweden
[c] Institute of Biochemistry and Food Chemistry, Food Chemistry Division, University of Hamburg, Grindelallee 117, D-20146 Hamburg, Germany
[d] Anterio Consult & Research GmbH, Augustaanlage 23, 68165 Mannheim, Germany
[e] Lehrstuhl für Biologische Chemie, Technische Universität München, 85350 Freising-Weihenstephan, Germany

ARTICLE INFO

Article history:
Received 8 January 2010
Revised 24 March 2010
Accepted 25 March 2010
Available online 8 April 2010

Keywords:
Mycobacterium tuberculosis
Lumazine synthase
Inhibitor
Virtual screening

ABSTRACT

Virtual screening of a library of commercially available compounds versus the structure of *Mycobacterium tuberculosis* lumazine synthase identified 2-(2-oxo-1,2-dihydrobenzo[*cd*]indole-6-sulfonamido)acetic acid (**9**) as a possible lead compound. Compound **9** proved to be an effective inhibitor of *M. tuberculosis* lumazine synthase with a K_i of 70 μM. Lead optimization through replacement of the carboxymethylsulfonamide sidechain with sulfonamides substituted with alkyl phosphates led to a four-carbon phosphate **38** that displayed a moderate increase in enzyme inhibitory activity (K_i 38 μM). Molecular modeling based on known lumazine synthase/inhibitor crystal structures suggests that the main forces stabilizing the present benzindolone/enzyme complexes involve π–π stacking interactions with Trp27 and hydrogen bonding of the phosphates with Arg128, the backbone nitrogens of Gly85 and Gln86, and the side chain hydroxyl of Thr87.

1. Introduction

Riboflavin (vitamin B2) plays a crucial role in many biological processes, including photosynthesis and mitochondrial electron transport. Riboflavin is biosynthesized by plants and numerous microorganisms but not by animals. Whereas animals obtain riboflavin from dietary sources, certain microorganisms such as Gram-negative pathogenic bacteria and yeasts lack efficient riboflavin uptake systems and are therefore absolutely dependent on endogenous riboflavin biosynthesis.[1–4] Riboflavin biosynthesis is therefore an attractive target for the design and synthesis of new antibiotics, which are urgently needed because pathogens are becoming drug resistant at an alarming rate. Lumazine synthase and riboflavin synthase catalyze the last two steps in the biosynthesis of riboflavin **(4)** (Scheme 1). The biosynthetic pathway starts off from one molecule of GTP,[5–7] which is converted to 5-amino-6-ribitylamino-2,4(1*H*,3*H*)-pyrimidinedione (**1**) by a sequence of ring opening, deamination, reduction, and dephosphorylation.[8–10] Lumazine synthase catalyzes the condensation of 3,4-dihydroxy-2-butanone 4-phosphate (**2**) with 5-amino-6-ribitylamino-2,4-(1*H*,3*H*)pyrimidinedione (**1**) yielding 6,7-dimethyl-8-D-ribityllumazine (**3**).[11–25] The final process in the biosynthesis of riboflavin (**4**) involves a mechanistically unusual dismutation of two molecules of 6,7-dimethyl-8-D-ribityllumazine (**3**) that results in the formation of one molecule of riboflavin and one molecule of the pyrimidinedione derivative **1**.[26–30]

Although the precise details remain to be established, the lumazine synthase-catalyzed reaction most likely proceeds along a mechanistic pathway involving formation of the Schiff base **5**, phosphate elimination affording **6**, tautomerization to **7**, ring closure, and dehydration to yield the lumazine **3** (Scheme 2).[31] Variations of this mechanism are possible depending on the Schiff base geometry and possible isomerization, conformational changes, and the timing of phosphate elimination.

Screening drug-like compounds by computational docking against the structure of a known target has become a promising avenue in lead discovery.[32–34] This approach is arguably much cheaper than experimental high-throughput screening and has been validated in other lead discovery projects.[35,36] The successful history of lumazine synthase structure determination and inhibitor development provides a sound basis for the selection of lead compounds from commercial chemical libraries and possible structural modification in order to improve the binding properties. The

* Corresponding author. Tel.: +1 765 494 1465; fax: +1 765 494 6790.
E-mail address: cushman@pharmacy.purdue.edu (M. Cushman).

0968-0896/$ - see front matter © 2010 Elsevier Ltd. All rights reserved.
doi:10.1016/j.bmc.2010.03.072

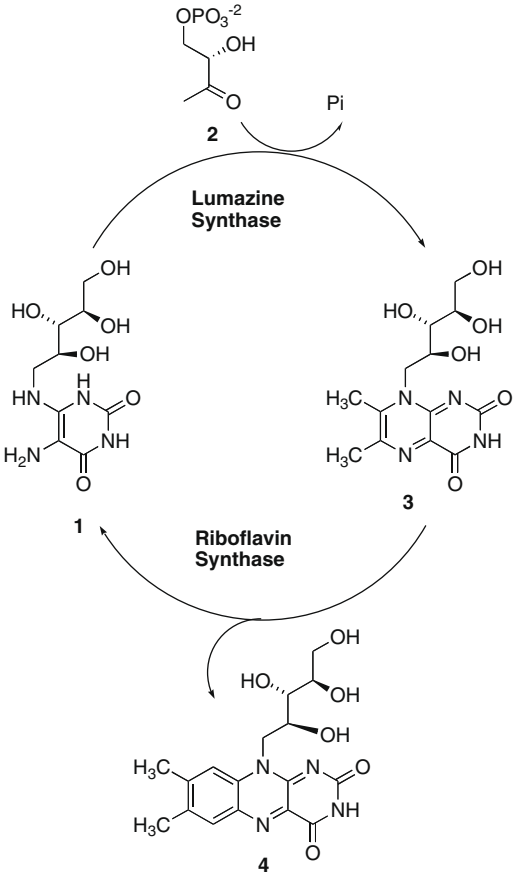

Scheme 1.

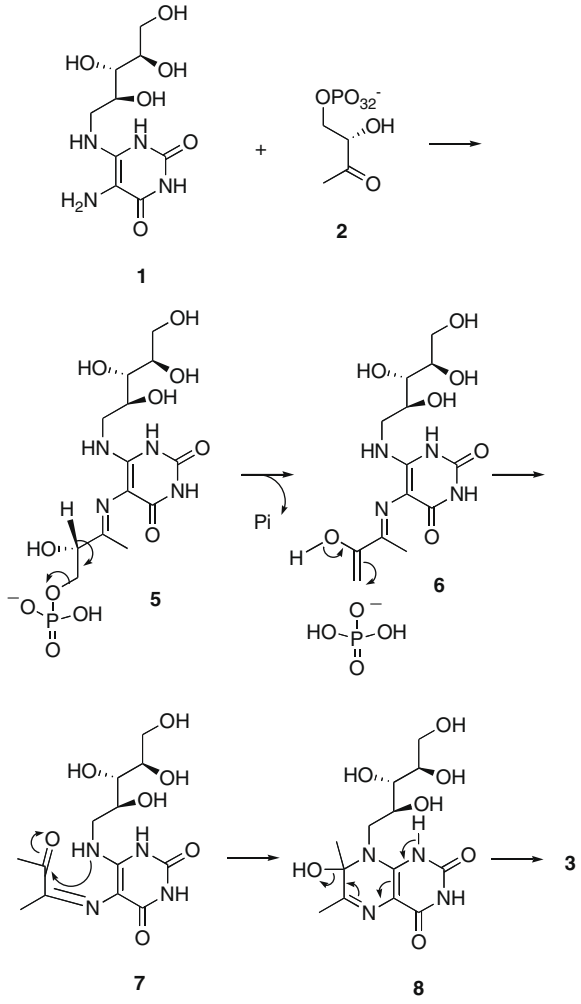

Scheme 2.

design of most of the known inhibitors of lumazine synthase has been based on the structures of both substrates of lumazine synthase and the putative Schiff base intermediate in the enzymatic reaction.[37,38]

The ZINC database,[39] maintained by the Shoichet group at UCSF, was subjected to virtual screening for the discovery of new lumazine synthase inhibitors. Docking the structures into the lumazine synthase structure led to an interesting new scaffold, compound **9** (Fig. 1), which has 'drug-like' features, such as a sulfonamide moiety, and therefore has more potential for drug development than mechanism-based probes containing polar ribityl side chains. The lead compound **9** displayed a K_i of 70 μM versus *Mycobacterium tuberculosis* lumazine synthase. It consists of an aromatic oxobenzindole ring system and a carboxymethylsulfonamide side chain. The inhibitor **9** lacks any close analogy to the pyrimidinedione ring or the ribityl side chain of the substrate **1**, which explains its relatively low affinity for the enzyme. However, it has been recently demonstrated that the ribityl chain present in the substrate, which was thought to be necessary for binding to the enzyme, can be replaced by a simple hydroxybenzylidene moiety (compound **12**) with retention of lumazine synthase inhibitory activity.[40] Moreover, it has recently been shown that the attachment of aliphatic chains bearing phosphate or phosphonate groups on the heterocyclic core dramatically increases binding affinity of the inhibitors.[41–45] An alkylphosphate chain consisting of 4–5 carbon atoms produces the strongest inhibitory effect. It therefore seemed logical to replace the carboxymethyl group of the lead compound **9** with alkyl phosphate groups and test the influence of the length of aliphatic chains with 2–6 carbon atoms. The rationale behind this design is that the phosphate moieties in compounds of general structure

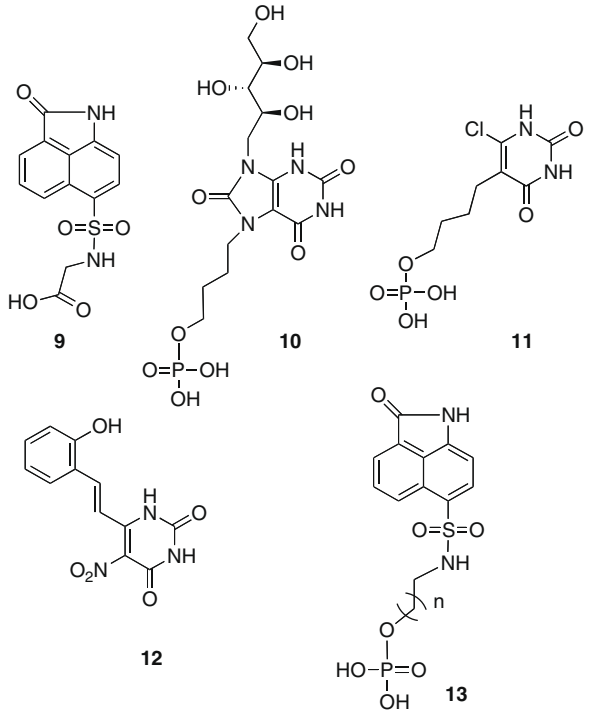

Figure 1. Representative *M. tuberculosis* lumazine synthase Inhibitors.

113 are expected to bind in the same phosphate binding pocket as the inhibitors **10** and **11**.

2. Results and discussion

2.1. Virtual screening

Virtual screening aims to discover inhibitors with novel scaffolds. In the present case, more than one million compounds were screened from the ZINC database,[39] which has been prepared for docking screening. The *M. tuberculosis* lumazine synthase crystal structure in complex with the inhibitor 3-(1,3,7-trihydro-9-D-ribityl-2,6,8-purinetrione-7-yl) propane 1-phosphate (PDB: 1w19) was prepared using Protein Preparation tools in Maestro 7.5 (Schrödinger LLC, Portland, Oregon), removing all crystal water molecules. The compounds were first docked with Glide 4.0 (Schrödinger LLC, Portland, Oregon) High Throughput Virtual Screening mode without any constraints.[46] A multi-stage screening workflow was applied, increasing the ligand conformational search and applying different scoring functions in order to rapidly reduce the number of possible hits. During the latter two stages of the screening, the following pharmacophore constraints were applied: three backbone hydrogen bonds to Ile83, Val81, Ala59 and the phosphate interaction to Arg128. At least three of these constraints had to be satisfied. The backbone hydrogen bonds are desirable because they could prevent future drug resistance issues. Based on solubility criteria posed by the ITC measurement, a solubility filter was also applied in the workflow. The cutoff score of −10 was chosen based on docking of several known active compounds[41] under the same conditions. The resulting 44 ligands were manually inspected and based on the interactions and their chemical scaffold, 12 compounds with different chemical scaffolds in total were selected for assay. Of these compounds, compound **9** demonstrated inhibition in the subsequent kinetic assay (Table 1). The principal of docking/pharmacophore based filtering is that it selects compounds complementary to the targeted site. Therefore, statistically, there is a much higher probability that the compounds selected by such a screening protocol will bind at the targeted site.

A straightforward synthesis (Scheme 3) was proposed for compounds having general structure **13**. The synthesis started from commercially available benz[*cd*]indol-2(1*H*)-one (**14**), which on treatment with chlorosulfonic acid yielded compound **15**.[47]

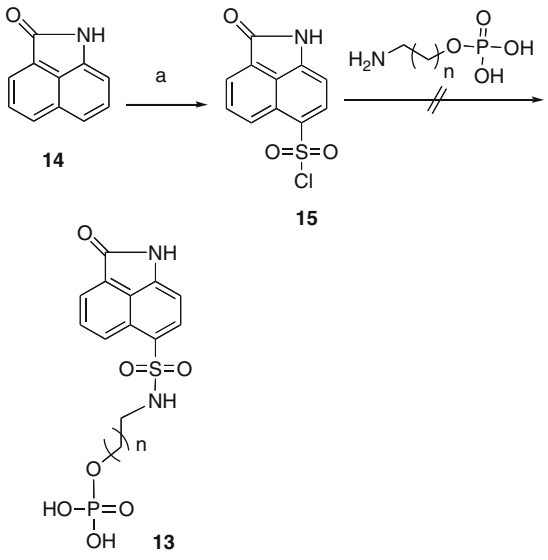

Scheme 3. Reagent and condition: (a) $ClSO_3H$, 0 °C.

Various procedures were tried unsuccessfully to produce the final compound **13**. The solvent system, base and temperature were varied without any improvement in results. The phosphate group was therefore protected before performing the coupling reaction. The syntheses of compounds **26** and **27** were both carried out the same way starting with the appropriate amino alcohol. Accordingly, the synthesis was started from ethanolamine (**16**), which on Cbz protection provided compound **18** (Scheme 4). The phosphate functionality in compound **20** was introduced by treatment of **18** with di-*tert*-butyl diisopropyl phosphoramidite under 1-*H* tetrazole catalysis, followed by in situ oxidation with hydrogen peroxide.[48,49] The Cbz group of compound **20** was removed via hydrogenolysis with Pd/C to afford the free amine compound **22**. Reaction of compound **15** with the free amine **22** in the presence of triethylamine provided the sulfonamide **24**. Subsequent deprotection of the phosphate with trifluoroacetic acid provided the desired product **26**.[50]

Scheme 4 was shortened by removing the Cbz protection step and the subsequent deprotection by hydrogenation. The improved

Table 1
Inhibition of recombinant riboflavin synthase (RS) and/or lumazine synthase (LS) of *M. tuberculosis* by selected compounds[a]

Compd	Enzyme	K_s[b] (μM)	K_{cat}[c] (m^{-1})	K_i[d] (μM)	K_{is}[e] (μM)	Mechanism
9	LS			70	58	
26	LS	9.8 ± 0.5	0.41 ± 0.01	260 ± 109	125 ± 57	Partial
	RS	5.7 ± 0.04	0.30 ± 0.01		>1000	
27	LS	15 ± 2	0.45 ± 0.01	99 ± 30	434 ± 115	Mixed
	RS	5.6 ± 0.04	0.28 ± 0.01		>1000	
38	LS	11 ± 1	0.44 ± 0.01	38 ± 8	572 ± 210	Mixed
	RS	6.5 ± 0.3	0.29 ± 0.01		>1000	
39	LS	19 ± 1	0.45 ± 0.01		563 ± 56	Uncompetitive
	RS	9.8 ± 0.6	0.56 ± 0.01		971 ± 179	Uncompetitive
40	LS	18 ± 1	0.45 ± 0.01		723 ± 91	Uncompetitive
	RS	9.8 ± 0.6	0.56 ± 0.01		898 ± 187	Uncompetitive
72	LS	16 ± 1	0.57 ± 0.01	832 ± 418	518 ± 94	Mixed
	RS	4.1 ± 0.3	0.15 ± 0.01		>1000	
77	LS	21 ± 2	0.61 ± 0.02	832 ± 418	>1000	Mixed
	RS	7.8 ± 0.3	0.34 ± 0.01		897 ± 104	Uncompetitive

Compounds **31**–**33**, **54**–**55**, **71**, **73**, **79** are not listed in this table since they did not significantly inhibit either lumazine synthase or riboflavin synthase.

[a] The assays with lumazine synthase were performed with dihydroxybutanone phosphate substrate held constant, while the concentration of the pyrimidinedione substrate was varied.

[b] K_s is the substrate dissociation constant for the equilibrium $E + S \rightleftharpoons ES$.

[c] K_{cat} is the rate constant for the process $ES \rightleftharpoons E + P$.

[d] K_i is the inhibitor dissociation constant for the process $E + I \rightleftharpoons EI$.

[e] K_{is} is the inhibitor dissociation constant process $ES + I \rightleftharpoons ESI$.

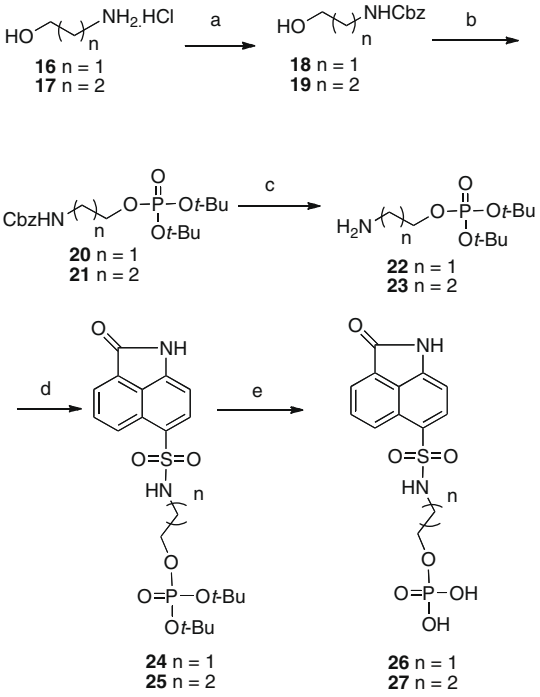

Scheme 4. Reagents and conditions: (a) benzylchloroformate, Et_3N, CH_2Cl_2, rt; (b) iPr$_2$NP(O^{t}Bu)$_2$, H_2O_2, tetrazole, rt; (c) H_2, Pd/C, MeOH; (d) **15**, Et_3N, THF, rt; (e) TFA, CH_2Cl_2, rt.

synthesis of oxobenzindole derivatives is outlined in Scheme 5. Simply mixing compound **15** with the respective amino alcohols in THF at room temperature provided the required intermediates **31–34** (Scheme 5). The phosphate group was introduced by treatment with di-*tert*-butyl diisopropyl phosphoramidite under tetrazole catalysis, followed by in situ oxidation with hydrogen peroxide to provide compounds **24** and **35–37**. The final deprotection of the *tert*-butyl groups with trifluoroacetic acid produced the required substances **26**, **38**, **39** and **40** with different linker chain lengths between the phosphate group and the sulfonamide moiety.

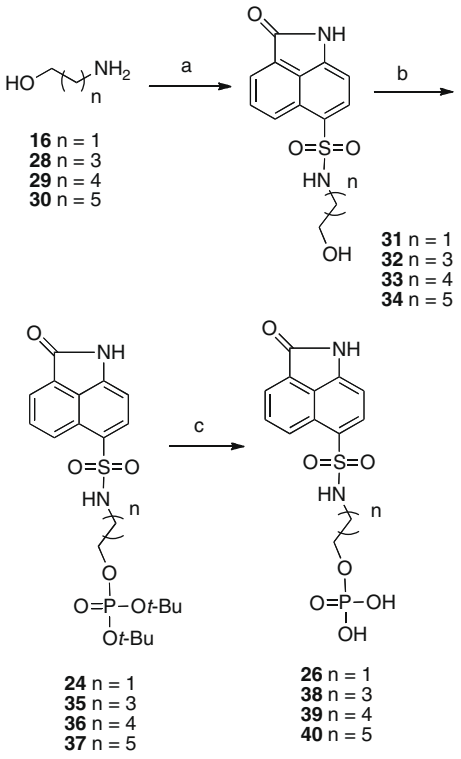

Scheme 5. Reagents and conditions: (a) **15**, Et_3N, THF, rt; (b) iPr$_2$NP(O^{t}Bu)$_2$, H_2O_2, tetrazole, rt; (c) TFA, CH_2Cl_2, rt.

Enzyme assays were performed with recombinant lumazine synthase and riboflavin synthase from *M. tuberculosis*. Assays with serial dilutions of each respective inhibitor were conducted in microtiter plates that were monitored photometrically over a period of 15 min. Data analysis was performed using Dynafit software.[51] Compound **38**, with a C-4 chain length, showed the best inhibitory activity (K_i of 38 μM) against *M. tuberculosis* lumazine synthase (Table 1). The inhibitory activity increases significantly as the connector chain length between the sulfonamide and phosphate groups is increased from two to four carbons.

The compounds studied had been designed to fit the active site of lumazine synthase. Since the product of lumazine synthase is the substrate of riboflavin synthase and there may be some similarity of the ligand recognition pattern of lumazine synthase and riboflavin synthase, the compounds under study were assayed versus the riboflavin synthase of *M. tuberculosis*. In fact, compounds **39**, **40**, and **77** were found to be weak, uncompetitive inhibitors of the enzyme with K_i values in the upper μM range (Table 1).

2.2. Molecular modeling of ligand binding to lumazine synthase

The X-ray crystal structure of the complex of 4-(6-chloro-2,4-dioxo-1,2,3,4-tetrahydropyrimidin-5-yl)butyl dihydrogen phosphate (**11**)[42] with lumazine synthase [PDB code: 2C97] with resolution 2.00 Å allowed the rational docking and energy minimization of newly synthesized compounds in the active site of *M. tuberculosis* lumazine synthase. Docking of the lead and synthesized compounds in the active site of *M. tuberculosis* lumazine synthase was performed with GOLD (BST, version 3.0, 2005). Energy minimization was performed with the MMFF94s force field in order to reduce steric clashes between the GOLD-docked compounds and the protein.

Figure 2 was constructed by displaying the amino acid residues of the enzyme involved in hydrogen bonding with the inhibitors **27** and **38** in the hypothetical model derived from docking and energy minimization. The maximum distance between the heavy atoms participating in the hydrogen bonds shown in Figure 2 was set at 3.8 Å. The binding patterns of both compounds are rather similar to each other and are comparable to that observed in the crystal structure of **11** in *M. tuberculosis* lumazine synthase. In general, the binding most likely reflects the contributions of the charged residue Arg128 and several polar residues that interact with the ligands directly via hydrogen bonding. The phosphate moiety of the ligands is extensively hydrogen bonded to the side chain nitrogens of Arg128, as well as the backbone nitrogens of Gly85 and Gln86 and the side chain hydroxyl of Thr87. Besides hydrogen bonding, the interaction of *M. tuberculosis* lumazine synthase and the inhibitor is predominantly hydrophobic. As expected, the calculated structural model positions the benzindolone aromatic rings of the ligands stacked with the indole ring of Trp27, consistent with the experimental structures of different lumazine synthase inhibitor complexes.[7,42,43,51–53] The carbonyl oxygen of the benzindolone moiety of both compounds hydrogen bonds with the backbone nitrogen of Ala59. Because of the longer aliphatic chain of **38**, the hydrophobic moiety of this compound is slightly shifted to the protein compared to the position of this moiety in the model with compound **27**. This shift results in formation of two additional hydrogen bonds by the carbonyl oxygen of the benzindolone moiety with the main chain nitrogen of Ile60 and with side chain oxygen of Glu61. Apparently, the formation of the additional hydrogen bonds is reflected in the better binding constant found for compound **38**.

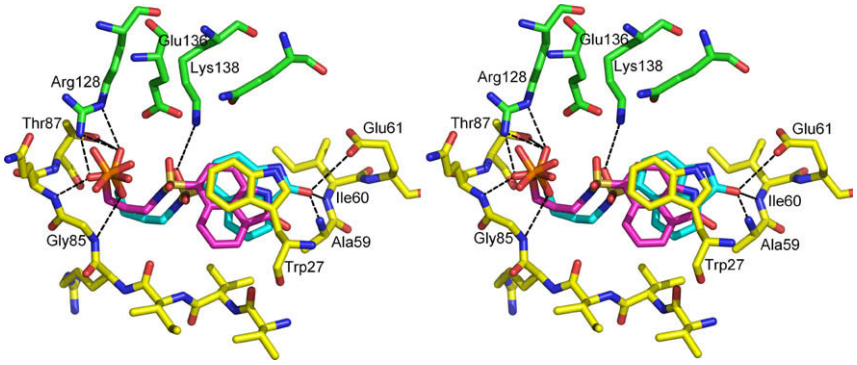

Figure 2. Structural representation of the hypothetical structure of compounds **27** and **38** bound in the active site of *M. tuberculosis* lumazine synthase. The amino acid residues involved in the active site are presented in ball and sticks and colored differently for two different subunits. The carbonyl atoms are shown in yellow and green, and nitrogen and oxygen atoms are shown in blue and red, respectively. The respective inhibitor molecules are colored in magenta (C3-alkylphosphate **27**) and cyan (C4-alkylphosphate **38**). The black dashed lines represent the putative interactions between compounds **38** and enzyme molecules. This figure was generated by PyMol [DeLano, W. L. (2002), the PyMOL Molecular Graphics System, DeLano Scientific, San Carlos, CA, USA] and programmed for wall-eyed (relaxed) viewing.

Comparison of these models with the known structures of *M. tuberculosis* lumazine synthase in complex with different substrate **1** analogues showed the lack of five hydrogen bonds involving the ribityl chains of the substrate **1** analogues,[43,54] and at least three hydrogen bonds formed between oxygen/nitrogen atoms of heterocyclic rings of the substrate **1** analogues and main/side chain atoms of Val81, Ile83 and Trp27 (Fig. 3). Trp27 is involved in binding through π–π stacking interactions. The hydrogen bonds involving the heterocyclic rings of the substrate **1** analogues seem to be particularly important for the affinities of the substrate analogues. For instance, the earlier discovered inhibitor **11**,[42,44] which also lacks the ribityl chain but contains oxygen/nitrogen substitutions in the heterocyclic ring, demonstrated very high inhibitory activity with an inhibition constant in the nanomolar range. The lumazine synthase inhibitory activities displayed by the benzindolone derivatives, which lack both a ribityl side chain and a pyrimidinedione system, are therefore surprising.

2.3. Thermodynamic characterization of binding

The apparent thermodynamic binding characteristics of compounds **26**, **27**, **38**, **39** and **40** were obtained by Isothermal Titration Calorimetry (ITC). Analysis of the changes in heat accompanying the binding reaction allowed the binding enthalpy of the processes (ΔH) to be derived, the stoichiometry (n) and association constants (K_a) to be estimated, and the entropy (ΔS) and free energy (ΔG) of the binding reactions to be calculated. Figure 4 shows a typical calorimetric titration of *M. tuberculosis* lumazine synthase in 100 mM potassium phosphate buffer at pH 7.0 and 30 °C with the compound containing the benzindolone group and a C3- (**27**) or C4-alkylphosphate chain (**38**). Earlier crystallographic studies of lumazine synthase from various organisms (*Bacillus subtilis*, *Schizosaccharomyces pombe* and *Aquifex aeolicus*)[21,51,55] suggested that orthophosphate ions are sufficient for the stability of the pentameric assemblies and consequently for the activity of the protein. Moreover, all attempts to crystallize any lumazine synthase in a phosphate-free environment and to obtain the thermodynamic characteristics have ended unsuccessfully. Thus, we have been forced to run our experiments in phosphate buffer and would like to emphasize that we are dealing with a tertiary binding reaction involving a phosphate ion, an inhibitor molecule, and free enzyme. As a result, the association constants and the binding free energy derived from our ITC experiments should be considered as 'apparent' thermodynamic parameters. Fitting of the binding isotherm was achieved with a model using a 'single set of identical sites' assuming that each of the active sites in the pentameric assembly is occupied by one inhibitor molecule. Binding of both compounds is exothermic with negative changes in binding enthalpy, although the titration of compounds to the reference phosphate buffer showed endothermic changes in the system. In order to correct for compound dilution, the compound was injected into phosphate buffer and the dilution heat was subtracted from the reaction heat. The measured negative enthalpy changes of -7.6 ± 1.3 kcal mol^{-1} for C4-alkylphosphate afforded an apparent association constant of $7.7 \times 10^3 \pm 0.5 \times 10^3$ M^{-1} with stoichiometry 1 for the binding reaction, in agreement with the expected binding of one inhibitor molecule in each of the five active sites of the pentameric protein. The calculated entropy ΔS and free energy of binding ΔG were -7.2 cal mol^{-1} deg^{-1} and -5.4 kcal mol^{-1}, respectively, which showed that the binding reaction is favored enthalpically. The

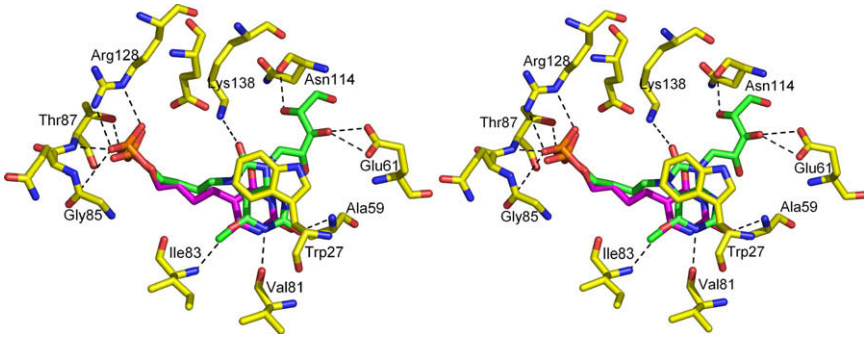

Figure 3. Crystal structure of **10** [PDB Code: 1W29] shown in green and **11** [PDB Code: 2C97] shown in pink bound to *M. tuberculosis* lumazine synthase. Hydrogen bonds formed by protein with the ribityl group, heterocyclic ring and phosphate group are shown for the compound **10.** The diagram is programmed for wall-eyed (relaxed) viewing.

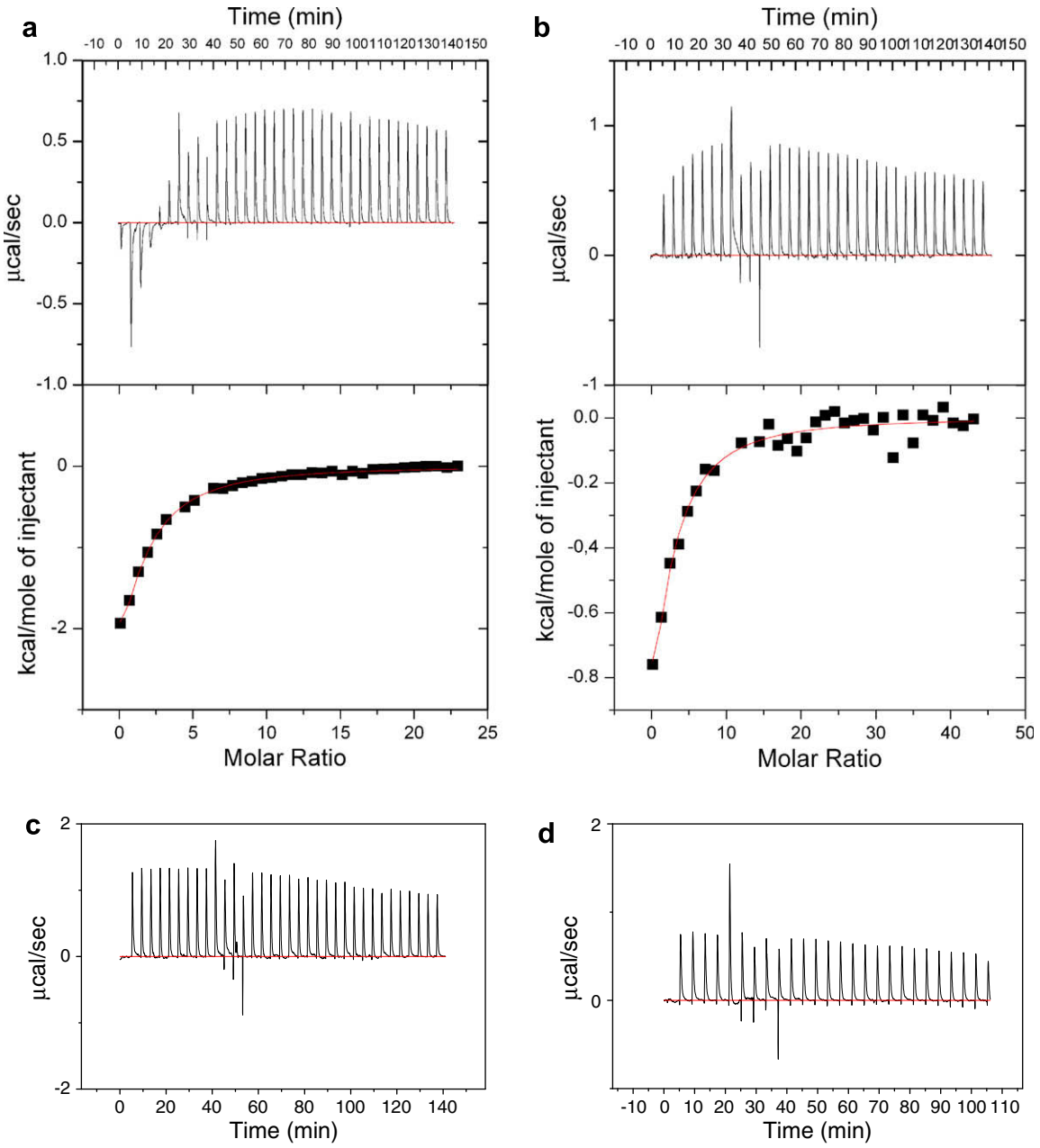

Figure 4. Calorimetric titration profiles of *M. tuberculosis* lumazine synthase with C4-alkylphosphate (**38**) (a) and C3-alkylphosphate (**27**) (b) at 30 °C. *Top panels.* Raw data obtained for 35 injections 8 µL each. The differential power signal recorded in the control titration of compound to the potassium phosphate buffer is presented on the insertions of top panels (a). *Bottom panels.* Integrated heat of binding reaction after subtraction of integrated heat of compound dilution plotted against molar ratio of total ligand concentration to total pentameric protein concentration. The solid line shows the best fit to the data, according to the model that assumes a single set of identical sites. For comparison, the titration calorimetry curves for lumazine synthase from *Bacillus anthracis* and *Schizosaccharomyces pombe,* respectively, titrated with C4-alkylphosphate compound **38** presented on panels (c) and (d) do not indicate a binding reaction.

measured enthalpy change for C3-alkylphosphate compound **27** was -5.2 ± 0.7 kcal mol^{-1}, which is less favorable than for C4-alkylphosphate compound **38**, but the loss in favorable enthalpy was compensated by a favorable positive entropy change ΔS of 0.98 cal mol^{-1} deg^{-1}. The resulting free energy of binding ΔG and apparent association constant K_a were -5.5 kcal mol^{-1} and $8.9 \times 10^3 \pm 3.5 \times 10^3$ M^{-1}, respectively. A similar enthalpy–entropy compensation effect was observed for the binding reaction of *M. tuberculosis* lumazine synthase **10**[43] and for the reaction of *Candida albicans* LS with **11**.[44]

Notably, the titration calorimetry experiments with **38** versus icosahedral lumazine synthase from *Bacillus anthracis* and the pentameric enzyme from *S. pombe* did not detect binding within the same experimental limits (Fig. 4). A structural comparison of the active sites of the enzymes showed a single mutation in *M. tuberculosis* lumazine synthase, G136E, which could be responsible for a different affinity to the ligands. Thus, the compounds produced in this study can be considered as specific ligands for *M. tuberculosis* enzyme and as leads for further development.

To determine the structural motif required for the activity, the intermediates **31**, **32** and **33** (Fig. 5) without the phosphate group were tested. They were found to be totally inactive. Although in the molecular modeling study the oxybenzindolone moieties were involved in π–π stacking interactions with Trp27, the compounds do not have any binding affinity in the active site. The evidence clearly

indicates that the phosphate group is necessary for the inhibitory activity.

To find metabolically stable inhibitors of *M. tuberculosis* lumazine synthase, compounds with phosphonate **41** and fluorophosphonate **42** moieties (Fig. 6) were synthesized with C-3, C-4 and C-5 chain length. Phosphonate and fluorophosphonate groups are stable to hydrolysis by phosphatases. The fluoro derivatives were synthesized because they more closely resemble the phosphate group electronically than the phosphonates do. The pK_a values of α,α-difluorophosphonates are closer to those of phosphates, while phosphonates are less acidic than phosphates. On the other hand, fluorophosphonates resemble phosphonates sterically (the van der Waals radii for fluorine and hydrogen are 1.35 and 1.20 Å, respectively).[56]

The synthesis (Scheme 6) started from diethylphosphite (**45**), which on treatment with 1,4-diiodobutane (**43**) and 1,5-diiodopentane (**44**) provided compounds **46** and **47**.[57,58] The iodo derivatives were converted to amines **50** and **51** via phthalimide derivatives **48** and **49**.[59,60] Treatment of benzindole sulfonyl chloride (Scheme 6) derivative **15** with amines **50** and **51** in THF provided the phosphonate derivatives **52** and **53**. The deprotection of the ethyl groups with TMSBr furnished the desired phosphonate derivatives **54** and **55**.

The phosphonate derivatives **54** and **55** showed absolutely no inhibitory activity. At physiological pH, the difference between the phosphate and phosphonate groups is that a phosphate group is mainly diionic and a phosphonate group is mainly monoionic.

The synthesis of the difluorophosphonates **64–66** is outlined in Scheme 7. After much effort, reagent **56** was converted to the required compound **57**.[61–64] Reaction of **56** with activated zinc dust[65]

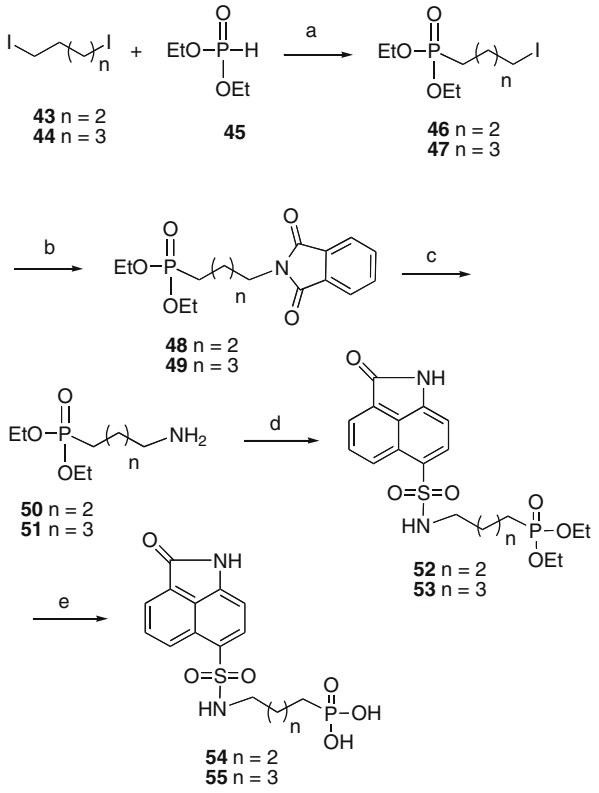

Scheme 6. Reagents and conditions: (a) NaH, THF, −20 °C 1 h then −10 °C 18h; (b) DMF, 100 °C; (c) $NH_2NH_2{\cdot}H_2O$, EtOH, reflux; (d) **15**, Et_3N, THF, rt; (e) TMSBr, CH_2Cl_2, rt.

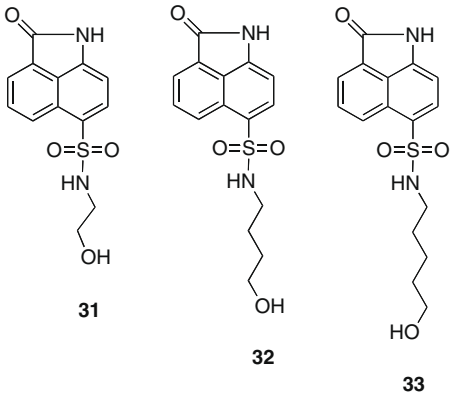

Figure 5.

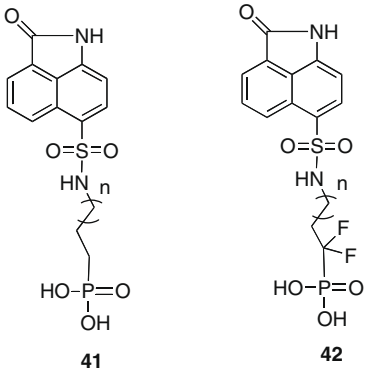

Figure 6. Compounds with phosphonate and fluorophosphonate moieties.

gave the stable [(diethoxyphosphinyl)difluoromethyl]zinc bromide, which on hydrolysis provided compound **57**.

Compound **57** when reacted at −78 °C with LDA in THF in the presence of hexamethylphosphoramide (HMPA) afforded a lithium anion, which was treated with diiodo compounds to provide the desired products **61**, **62** and **63** in approximately 20% yield. The poor yields observed in these reactions are probably due to the poor nucleophilicity of the highly stabilized lithium anion and its poor stability above −25 °C. Without HMPA, no alkylation was observed. An attempt was made to convert the iodo derivatives **61**, **62** and **63** to amines via the standard Gabriel procedure by making the phthalimide derivatives **64**, **65** and **66**, but mixtures of products were obtained that were very hard to separate and characterize. Thus, the reverse strategy was considered, and

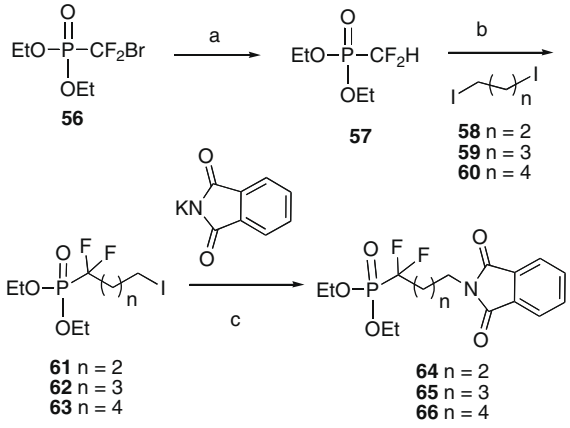

Scheme 7. Reagents and conditions: (a) (i) Zn, Et_2O, reflux; (ii) H_2O; (b) LDA, HMPA, −78 °C; (c) DMF, 100 °C.

accordingly, the sulfonyl chloride compound **15** was converted to the sulfonamide derivative **67** with ammonia in THF (Scheme 8).

Treatment of the sulfonamide derivative **67** with the iodo compounds **61**, **62** and **63** in the presence of K_2CO_3 (Scheme 8) provided the protected benzindolone fluorophosphonate derivatives **68**, **69** and **70**. Finally, the removal of the ethyl groups with TMSBr furnished the desired products **71**, **72** and **73** with fluorophosphonate groups. Surprisingly, the fluorophosphonate derivatives **71**, **72** and **73** turned out to be inactive against *M. tuberculosis* lumazine synthase and *M. tuberculosis* riboflavin synthase, except for compound **72**, which showed poor inhibitory activity against *M. tuberculosis* lumazine synthase (Table 1). Compound **72** corresponds to compound **38**, bearing an alkylphosphate chain consisting of 4 carbon atoms, which exhibited the strongest enzyme inhibitory effect. Evidently, in this particular case, phosphonates and fluorophosphonates proved to be very poor mimics of the phosphate group of the inhibitors, although in other cases involving lumazine synthase, they were effective.[41,66,67]

The mechanism outlined in Scheme 2 is certainly reasonable, but questions still remain about the timing of phosphate elimination relative to the conformational reorganization of the side chain. Nevertheless, it is clear that the inorganic phosphate must eventually be released at some point to make way for new substrate. As mentioned above, the benzindolone moiety by itself does not have significant binding affinity considering that compounds **31**, **32** and **33** are totally inactive. On the other hand, the active phosphates must be able to displace inorganic phosphate from the phosphate binding pocket for any inhibitory activity and therefore the non-phosphate part of their structures must contribute positively in this regard. Compound **11**, with a C-4 chain length, showed strong inhibitory activity (K_i 0.88 μM) against *M. tuberculosis* lumazine synthase. Compounds **77** and **79**, which lack the phosphate group, were synthesized (Scheme 9). As expected, compounds **77** and **79** were inactive. This substantiates the point that although the pyrimidinedione ring alone does not have any binding affinity; it contributes positively to the binding of compound **11**, since its phosphate group displaces inorganic phosphate from the phosphate binding pocket. The highlights of the synthesis of compounds **77** and **79** were the selective reduction of the nitro group to an amino group with sodium dithionate, and the removal of benzyl protecting groups under controlled hydrogenolysis using 1,4-cyclohexediene as a source of hydrogen.

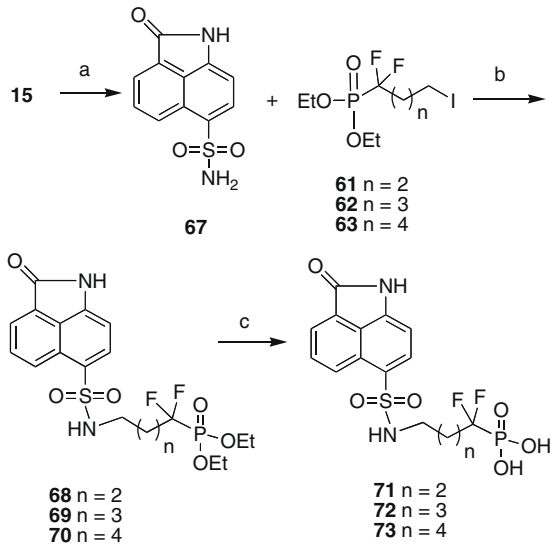

Scheme 8. Reagents and conditions: (a) NH_3, THF, rt; (b) K_2CO_3, THF, rt; (c) TMSBr, CH_2Cl_2, rt.

Compounds **27** and **38**, with C-3 and C-4 alkyl phosphate chains, showed better inhibitory activity against *M. tuberculosis* lumazine synthase. The inhibitory activity increases significantly with an increase in the alkyl phosphate chain length connector between sulfonamide and phosphate groups from two carbons to four carbons, but then the inhibitory activity decreases as the chain length increases. The expected pK_a of the phosphonate derivatives **54** and **55** suggest that these derivatives are mainly monoionic, thus, they are unable to displace the inorganic phosphate. Although the fluorophosphonate derivatives **71**, **72** and **73** have favorable pK_a values, it seems they are also unable to displace the inorganic phosphate from the phosphate binding pocket. Fluorophosphonate derivative **72**, which corresponds to compound **38** bearing an alkyl phosphate chain consisting of four carbon atoms, showed some inhibitory activity against *M. tuberculosis* lumazine synthase, with K_i values of 832 μM and K_{is} 518 μM. Molecular modeling of fluorophosphonate–lumazine synthase complex did not reveal a structural basis for these unexpected findings.

To delve deeper into the nature of the phosphate binding site, information obtained by REDOR NMR spectroscopy of complexes of lumazine synthase from *Saccharomyces cerevisiae* with phosphonate reaction intermediate analogues **80** was used (Fig. 7).[45] The $^{15}N\{^{31}P\}$ REDOR NMR spectra of those complexes indicated that mobility of the Lys92 side chain could facilitate the required active site release of phosphate during the enzyme catalysis. Although the exact nature of the phosphate binding pocket still remains elusive, it is clear that the inorganic phosphate must be displaced by organic phosphate from the phosphate binding pocket for any enzyme inhibitory activity. These compounds have a pyrimidinedione ring and a ribityl side chain, which contribute to their affinity for lumazine synthase. The binding of oxybenzindolone compounds in the active site of lumazine synthase depends on their abilities to bind at the phosphate binding site. The metabolically stable fluorophosphonate derivative **72**, which showed moderate activity, could possibly be used as a ^{19}F NMR mechanistic probe to study the structure of the occupied phosphate binding sites of lumazine synthase.

In virtual screening, finding novel active scaffolds is the most important success criterion. The oxybenzindolone derivatives provide unique structural probes of the active site of lumazine syn-

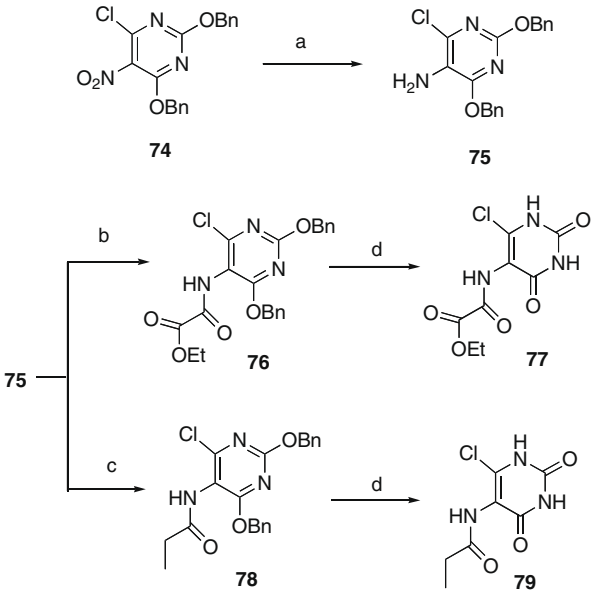

Scheme 9. Reagents and conditions: (a) $Na_2S_2O_4$, 1,4-dioxane, MeOH, buffer, reflux; (b) $ClCOCO_2Et$, Et_3N, THF, rt; (c) C_2H_5COCl, Et_3N, THF, rt; (d) Lindlar catalyst, 1,4-cyclohexadiene, ethanol, r.t.

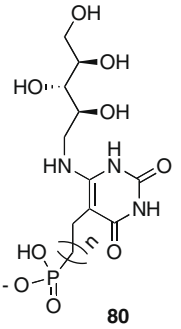

80

Figure 7. Phosphonate reaction intermediate analogues.

thase. The lead compound has 'drug-like' features and therefore has more potential for drug development than the mechanism probes containing polar ribityl side chains. Although the oxybenzindolone moiety has poor affinity to the active site, the enzyme inhibitory activity could possibly be optimized by improving the binding affinity of the oxybenzindolone moiety through incorporation of oxygen- or nitrogen-containing functional groups. Optimization of the enzyme inhibitory activity through logical structure manipulation of the lead compound **9** already provided compound **38** with moderately improved inhibitory activity (K_i 38 μM) against *M. tuberculosis* lumazine synthase.

3. Experimental

3.1. 2-Oxo-1,2-dihydrobenzo[*cd*]indole-6-sulfonyl chloride (15)

Chlorosulfonic acid (3.2 mL) was added slowly to compound **14** (1.0 g, 5.9 mmol). The reaction mixture was stirred at 0 °C for 1 h and at room temperature for 2 h. The mixture was then poured into ice water (20 mL). The precipitate was washed with water (2 × 10 mL) and dried to give compound **15** as yellow solid (0.76 mg, 44%): mp 143–146 °C. ^{1}H NMR (300 MHz, MeOH-d_4) δ 10.34 (br s, 1H), 8.68 (d, J = 8.3 Hz, 1H), 8.38 (d, J = 7.9 Hz, 1H), 8.20 (d, J = 7.0 Hz, 1H), 8.12 (dd, J = 7.0 Hz, 8.3 Hz, 1H), 7.22 (d, J = 7.9 Hz, 1H); ^{13}C NMR (75 MHz, MeOH-d_4) δ 169.0, 147.3, 135.5, 133.0, 132.5, 129.1, 128.0, 127.6, 126.5, 124.7, 105.2; EIMS *m/z* (rel intensity) 267 (M^+, 4), 232 (5), 155 (38), 91 ($C_5H_7^+$, 100); CIMS *m/z* (rel intensity) 268 (MH^+, 76), 232 (53), 197 (100). Anal. Calcd for $C_{11}H_6ClNO_3S$: C, 49.36; H, 2.26; N, 5.23; S, 11.98. Found: C, 49.53; H, 2.08; N, 5.47; S, 12.21.

3.2. Benzyl-2-(di-*tert*-butoxyphosphoryloxy)ethylcarbamate (20)

Tetrazole (3 wt % solution in CH_3CN, 32 mL, 11.0 mmol) and di-*tert*-butyl-*N,N*-diisopropylphosphoramidite (95%, 2.73 mL, 8.2 mmol) were added to a solution of benzyl-2-hydroxyethylcarbamate (**18**) (1.07 g, 5.48 mmol) in THF (20 mL) and the mixture was stirred at room temperature for 16 h. The mixture was cooled to 0 °C and H_2O_2 (70% aqueous, 1.0 mL, 24 mmol) was added. After 15 min, the cooling bath was removed and the mixture was stirred for a further 6 h, and then aqueous Na_2SO_3 (10%, 50 mL) was added with water bath cooling. After 25 min, the organic solvents were removed under reduced pressure and the aqueous residue was extracted with EtOAc (3 × 30 mL). The combined extracts were washed with brine, dried, and evaporated. The residue was purified by silica gel column chromatography, eluting with EtOAc–petroleum ether (1:1), to afford the product **20** (1.36 g, 64%) as a colorless oil. ^{1}H NMR (300 MHz, $CDCl_3$) δ 7.37–7.25 (m, 5H), 5.64 (br s, 1H), 5.03 (s, 2H), 3.96 (m, 2H), 3.38 (q, J = 5.1 Hz, 2H), 1.41 (s, 18H); ^{13}C NMR (75 MHz, $CDCl_3$) δ 156.3, 136.5, 128.1, 127.7, 82.2, 82.1, 66.1, 64.1, 37.3, 30.1, 29.9, 29.8, 29.5; EIMS *m/z* (rel intensity) 796 ($2MNa^+$, 100), 774 ($2M^+$, 94), 410 (MNa^+, 48), 388 (MH^+, 80); HRMS *m/z* calcd for $C_{18}H_{30}NO_6P$ (MH^+) 388.1889, found 388.1880.

3.3. Benzyl-2-(di-*tert*-butoxyphosphoryloxy)propylcarbamate (21)

Tetrazole (3 wt % solution in CH_3CN, 4.5 mL, 1.91 mmol) and di-*tert*-butyl-*N,N*-diisopropylphosphoramidite (95%, 0.45 mL, 1.43 mmol) were added to a solution of benzyl-2-hydroxypropylcarbamate (**19**) (200 mg, 0.96 mmol) in THF (5 mL) and the mixture was stirred at room temperature for 16 h. The mixture was cooled to 0 °C and H_2O_2 (70% aqueous, 0.4 mL, 24 mmol) was added. After 15 min, the cooling bath was removed and the mixture was stirred for a further 6 h, and then aqueous Na_2SO_3 (10%, 50 mL) was added with water bath cooling. After 25 min, the organic solvents were removed under reduced pressure and the aqueous residue was extracted with EtOAc (3 × 10 mL). The combined extracts were washed with brine, dried, and evaporated. The residue was purified by silica gel column chromatography, eluting with EtOAc–petroleum ether (1:1), to provide the product **21** (250 mg, 65%) as a colorless oil. ^{1}H NMR (300 MHz, $CDCl_3$) δ 7.24 (m, 5H), 5.76 (br s, 1H), 5.00 (s, 2H), 3.92 (m, 2H), 3.23 (m, 2H), 1.76 (m, 2H), 1.38 (s, 18H); ^{13}C NMR (75 MHz, $CDCl_3$) δ 156.2, 136.3, 128.2, 127.7, 82.5, 82.4, 66.3, 65.5, 41.1, 30.1, 29.51, 29.47; EIMS *m/z* (rel intensity) 825 ($2MNa^+$, 2), 424 (MNa^+, 100); HRMS *m/z* calcd for $C_{19}H_{32}NO_6P$ (MNa^+) 424.1865, found 424.1864.

3.4. Di-*tert*-butyl-2-(2-oxo-1,2-dihydrobenzo[*cd*]indole-6-sulfonamido)ethyl phosphate (24)

Method 1. A solution of **20** (1.17 g, 3.02 mmol) in MeOH (30 mL) with Pd/C (5%, 0.21 g) was hydrogenated at 50 psi for 4 h. The mixture was filtered through Celite, washed with MeOH (2 × 10 mL), and the filtrate was evaporated to give 2-aminoethyl di-*tert*-butyl phosphate (**22**) (604 mg, 79%) as colorless oil, which was used directly for the next reaction. A solution of amine **22** (100 mg, 0.39 mmol) and Et_3N (0.11 mL, 0.79 mmol) in THF (2 mL) was added to a solution of compound **15** (106 mg, 0.39 mmol) in THF (3 mL) at 0 °C. After 5 min, the cooling bath was removed and the reaction mixture was stirred overnight. The mixture was diluted with water and extracted with CH_2Cl_2 (3 × 15 mL). The combined extracts were dried and evaporated and the residue was purified by silica gel column chromatography, eluting with ethyl acetate–petroleum ether (9:1), to provide compound **24** (135 mg, 71%) as yellow solid: mp 200–203 °C. *Method 2.* Tetrazole (3 wt % solution in CH_3CN, 1.6 mL, 0.68 mmol) and di-*tert*-butyl-*N,N*-diisopropylphosphoramidite (95%, 0.16 mL, 0.51 mmol) were added to a solution of **31** (100 mg, 0.34 mmol) in THF (4 mL) and the mixture was stirred at room temperature for 16 h. The mixture was cooled to 0 °C and H_2O_2 (70% aqueous, 0.3 mL, 1.71 mmol) was added. After 15 min, the cooling bath was removed and the mixture was stirred for a further 6 h, and then aqueous Na_2SO_3 (10%, 5 mL) was added with water bath cooling. After 25 min, the organic solvents were removed under reduced pressure and the aqueous residue was extracted with EtOAc (3 × 10 mL). The combined extracts were washed with brine, dried, and evaporated. The residue was purified by silica gel column chromatography, eluting with EtOAc–petroleum ether (9:1), to give **24** (110 mg, 67%) as a as yellow solid: mp 200–203 °C. ^{1}H NMR (300 MHz, $CDCl_3$) δ 9.55 (br s, 1H), 8.68 (d, J = 8.4 Hz, 1H), 8.09 (d, J = 7.5 Hz, 1H), 8.03 (d, J = 7.0 Hz, 1H), 7.79 (m, 1H), 6.96 (d, J = 7.5 Hz, 1H), 6.34 (br s, 1H), 3.99 (m, 2H), 3.12 (m, 2H), 1.38 (s, 18H); ^{13}C NMR (75 MHz, $CDCl_3$) δ 169.8, 142.2, 132.7, 130.5, 130.0, 128.6, 126.8, 125.3, 124.9, 104.9, 83.4, 83.3, 65.6, 43.4, 29.7; negative ion EIMS *m/z* (rel intensity) 483 [$(M-H^+)^-$, 78], 464 (20), 276 (50); HRMS *m/z* calcd for $C_{21}H_{29}N_2O_7PS$ $(M-H^+)^-$ 483.1355, found 483.1348.

3.5. Di-*tert*-butyl-3-(2-oxo-1,2-dihydrobenzo[*cd*]indole-6-sulfonamido)propyl phosphate (25)

A solution of **21** (0.3 g, 0.75 mmol) in MeOH (30 mL) with Pd/C (5%, 20 mg) was hydrogenated at 50 psi for 4 h. The mixture was filtered through Celite, washed with MeOH (2 × 10 mL), and the filtrate was evaporated to give 2-aminopropyl di-*tert*-butyl phosphate (**23**) (140 mg, 70%) as colorless oil, which was used directly for the next reaction. A solution of amine **23** (100 mg, 0.37 mmol) and Et_3N (0.1 mL, 0.75 mmol) in THF (2 mL) was added to a solution of compound **15** (100 mg, 0.37 mmol) in THF (3 mL) at 0 °C. After 5 min, the cooling bath was removed and the reaction mixture was stirred overnight. The mixture was diluted with water and extracted with CH_2Cl_2 (3 × 15 mL). The combined extracts were dried and evaporated and the residue was purified by silica gel column chromatography, eluting with ethyl acetate–petroleum ether (9:1), to give compound **25** (112 mg, 60%) as yellow solid: mp 196–198 °C. ^{1}H NMR (300 MHz, acetone-d_6) δ 8.98 (d, J = 8.4 Hz, 1H), 8.39 (d, J = 7.5 Hz, 1H), 8.34 (d, J = 7.0 Hz, 1H), 8.18 (m, 1H), 7.35 (d, J = 7.5 Hz, 1H), 4.16 (dd, J = 6.3, 12.8 Hz, 2H), 3.26 (t, J = 6.9 Hz, 2H), 2.03 (m, 2H), 1.62 (s, 18H); ^{13}C NMR (75 MHz, acetone-d_6) δ 169.2, 142.4, 132.4, 130.1, 129.4, 128.6, 126.8, 126.5, 124.7, 124.4, 104.2, 81.8, 81.7, 63.8, 63.7, 39.1, 29.9; EIMS *m/z* (rel intensity) 521 (MNa^+, 92), 499 (MH^+, 100), 387 (62); negative ion EIMS *m/z* (rel intensity) 995 [$(2M-H^+)^-$, 34], 533 (100), 497 [$(M-H^+)^-$, 91]; HRMS *m/z* calcd for $C_{22}H_{31}N_2O_7PS$ 521.1487 (MNa^+), found 521.1492.

3.6. 2-(2-Oxo-1,2-dihydrobenzo[*cd*]indole-6-sulfonamido)ethyl dihydrogen phosphate (26)

TFA (0.06 mL, 0.8 mmol) was added to a solution of **24** (40 mg, 0.083 mmol) in CH_2Cl_2 (5 mL) and the solution was allowed to stand at room temperature for 16 h. The mixture was evaporated, and the residue was washed with CH_2Cl_2 (3 × 10 mL) and dried to yield **26** (23 mg, 74%) as a light-yellow solid: mp 185–188 °C. ^{1}H NMR (300 MHz, MeOH-d_4) δ 8.72 (d, J = 8.4 Hz, 1H), 8.14 (d, J = 7.5 Hz, 1H), 8.10 (d, J = 7.0 Hz, 1H), 7.92 (m, 1H), 7.05 (d, J = 7.5 Hz, 1H), 3.89 (dd, J = 6.0, 13.0 Hz, 2H), 3.13 (t, J = 5.8 Hz, 2H); ^{13}C NMR (75 MHz, MeOH-d_4 and DMSO-d_6) δ 169.1, 142.7, 132.7, 130.8, 129.9, 128.6, 127.1, 126.5, 125.1, 124.7, 104.9, 64.0, 42.9; EIMS *m/z* (rel intensity) 395 (MNa^+, 25), 373 (MH^+, 100), 338 (37), 293 (26), 274 (21); negative ion EIMS *m/z* (rel intensity) 743 [$(2M-H^+)^-$, 100], 371 [$(M-H^+)^-$, 51], 236 (10); HRMS *m/z* calcd for $C_{13}H_{13}N_2O_7PS$ (MH^+) 373.0259, found 373.0252. Anal. Calcd for $C_{13}H_{13}N_2O_7PS{\cdot}1.5H_2O$: C, 39.10; H, 4.04; N, 7.02; P, 7.76. Found: C, 39.15; H, 3.73; N, 7.02; P, 7.89.

3.7. 3-(2-Oxo-1,2-dihydrobenzo[*cd*]indole-6-sulfonamido)propyl dihydrogen phosphate (27)

TFA (0.07 mL, 0.8 mmol) was added to a solution of **25** (40 mg, 0.081 mmol) in CH_2Cl_2 (5 mL) and the solution was allowed to stand at room temperature for 16 h. The mixture was evaporated, the residue was washed with CH_2Cl_2 (3 × 10 mL), and the product was dried to provide **27** (21 mg, 68%) as a light-yellow solid: mp 192–195 °C. ^{1}H NMR (300 MHz, MeOH-d_4) δ 8.65 (d, J = 8.4 Hz, 1H), 8.07 (d, J = 7.6 Hz, 1H), 8.01 (d, J = 7.0 Hz, 1H), 7.84 (m, 1H), 7.00 (d, J = 7.6 Hz, 1H), 3.91 (dd, J = 6.3, 12.8 Hz, 2H), 2.97 (t, J = 6.8 Hz, 2H), 1.75 (m, 2H); ^{13}C NMR (75 MHz, MeOH-d_4) δ 171.4, 143.8, 133.8, 131.5, 131.0, 130.1, 128.1, 127.8, 126.1, 106.1, 64.8, 40.4, 31.7; EIMS *m/z* (rel intensity) 387 (MH^+, 100), 338 (3), 311 (3); negative ion EIMS *m/z* (rel intensity) 771 [$(2M-H^+)^-$, 100], 385 [$(M-H^+)^-$, 36]; HRMS *m/z* calcd for $C_{14}H_{15}N_2O_7PS$ (MH^+) 387.0416, found 387.0419. Anal. Calcd for $C_{14}H_{15}N_2O_7PS{\cdot}H_2O$: C, 41.59; H, 4.24; N, 6.93. Found: C, 41.35; H, 4.31; N, 6.99.

3.8. *N*-(2-Hydroxyethyl)-2-oxo-1,2-dihydrobenzo[*cd*]indole-6-sulfonamide (31)

Ethanolamine (0.05 mL, 0.84 mmol) was added to solution of compound **15** (150 mg, 0.56 mmol) in THF (5 mL) and the reaction mixture was stirred at room temperature for 12 h. THF was removed under vacuum and the residue was purified by silica gel column chromatography, eluting with EtOAc–petroleum ether (4:6), to give compound **31** (115 mg, 70%) as yellow solid: mp 192–195 °C. ^{1}H NMR (300 MHz, MeOH-d_4) δ 8.72 (d, J = 8.4 Hz, 1H), 8.12 (d, J = 7.5 Hz, 1H), 8.10 (d, J = 6.8 Hz, 1H), 7.90 (m, 1H), 7.04 (d, J = 7.5 Hz, 1H), 3.48 (t, J = 6.0 Hz, 1H), 2.95 (d, J = 6.0 Hz, 1H); ^{13}C NMR (125 MHz, MeOH-d_4) δ 171.1, 144.2, 134.1, 132.3, 132.2, 131.0, 128.1, 128.0, 126.5, 106.4, 61.8, 45.9; EIMS *m/z* (rel intensity) 315 (MNa^+, 85), 293 (MH^+, 42); negative ion EIMS *m/z* (rel intensity) 291 [$(M-H^+)^-$, 10], 248 (100); HRMS *m/z* calcd for $C_{13}H_{12}N_2O_4S$ (MNa^+) 315.0416, found 315.0420.

3.9. *N*-(2-Hydroxybutyl)-2-oxo-1,2-dihydrobenzo[cd]indole-6-sulfonamide (32)

4-Amino-1-butanol (**28**) (0.08 mL, 0.84 mmol) was added to solution of compound **15** (150 mg, 0.56 mmol) in THF (5 mL) and the reaction mixture was stirred at room temperature for 12 h. THF was removed under vacuum and the residue was purified by silica gel column chromatography, eluting with EtOAc–petroleum ether (4:6), to give compound **32** (120 mg, 67%) as yellow solid: mp 238–240 °C. ^{1}H NMR (300 MHz, MeOH-d_4) δ 8.73 (d, J = 8.2 Hz, 1H), 8.12 (d, J = 7.6 Hz, 1H), 8.11 (d, J = 6.9 Hz, 1H), 7.90 (dd, J = 7.1, 8.4 Hz, 1H), 7.04 (d, J = 7.6 Hz, 1H), 3.39 (t, J = 6.0 Hz, 1H), 2.87 (d, J = 6.6 Hz, 1H), 1.42 (m, 4H); ^{13}C NMR (75 MHz, MeOH-d_4) δ 171.5, 143.9, 133.8, 131.5, 131.1, 130.7, 128.1, 126.3, 126.2, 106.0, 62.2, 43.7, 30.6, 27.1; EIMS *m/z* (rel intensity) 321 (MH^+, 83), 283 (34); negative ion EIMS *m/z* (rel intensity) 639 [$(2M-H^+)^-$, 66], 319 [$(M-H^+)^-$, 100], 248 (79); HRMS *m/z* calcd for $C_{15}H_{16}N_2O_4S$ (MH^+) 321.0909, found 321.0911.

3.10. *N*-(5-Hydroxypentyl)-2-oxo-1,2-dihydrobenzo[*cd*]indole-6-sulfonamide (33)

5-Amino-1-pentanol (**29**) (0.3 g, 2.9 mmol) was added to a solution of compound **15** (200 mg, 0.75 mmol) in THF (5 mL) and the reaction mixture was stirred at room temperature for 24 h under argon gas. THF was removed under vacuum and yellow solid was purified using silica gel column chromatography, eluting with MeOH–EtOAc (8:92) to provide compound **33** (180 mg, 70%) as a yellow solid: mp 186–189 °C. ^{1}H NMR (300 MHz, MeOH-d_4) δ 8.71 (d, J = 8.4 Hz, 1H), 8.10 (d, J = 7.5 Hz, 1H), 8.09 (d, J = 6.9 Hz, 1H), 7.89 (t, J = 8.3 Hz, 1H), 7.04 (d, J = 7.6 Hz, 1H), 3.36 (t, J = 6.4 Hz, 2H), 2.85 (t, J = 6.8 Hz, 2H), 1.35 (m, 4H), 1.22 (m, 2H); ^{13}C NMR (75 MHz, MeOH-d_4) δ 171.3, 143.9, 133.8, 131.4, 131.1, 130.7, 128.3, 128.0, 126.1, 105.9, 62.6, 43.7, 32.9, 30.3, 23.8; negative ion ESIMS *m/z* (rel intensity) 667 ([$2M-H^+$]$^-$, 100), 333 ([$M-H^+$]$^-$, 45); HRMS *m/z* calcd for $C_{16}H_{18}N_2O_4S$ (MH^+) 335.1066, found 335.1063.

3.11. *N*-(6-Hydroxyhexyl)-2-oxo-1,2-dihydrobenzo[*cd*]indole-6-sulfonamide (34)

6-Amino-1-hexanol (**30**) (315 mg, 2.69 mmol) was added to a solution of compound **15** (180 mg, 0.672 mmol) in THF (7 mL) and the mixture was allowed to stir overnight. THF was removed under vacuum and the residue was purified using silica gel column chromatography, eluting with EtOAc–hexane (8:2) and then MeOH–EtOAc (5:95), to result in starting material **15** (72 mg)

and pure compound **34** as a yellow solid (100 mg, 45%): mp 190–192 °C. ^{1}H NMR (300 MHz, MeOH-d_4) δ 8.73 (d, J = 8.4 Hz, 1H), 8.12 (d, J = 7.6 Hz, 1H), 8.11 (d, J = 6.9 Hz, 1H), 7.91 (dd, J = 7.2, 8.3 Hz, 1H), 7.05 (d, J = 7.5 Hz, 1H), 3.39 (t, J = 6.5 Hz, 2H), 3.34 (s, 1H), 2.85 (t, J = 6.9 Hz, 2H), 1.33 (m, 4H), 1.13 (m, 4H); ^{13}C NMR (125 MHz, MeOH-d_4) δ 171.2, 143.5, 133.8, 131.2, 131.1, 130.0, 128.0, 127.9, 126.0, 105.5, 62.3, 43.7, 33.1, 30.5, 27.0, 26.5; ESIMS m/z (rel intensity) 371 (MNa^+, 51), 349 (MH^+, 100); negative ion ESIMS m/z (rel intensity) 695 ($[2M-H^+]^-$, 100), 347 ($[M-H^+]^-$, 47); HRMS m/z calcd for $C_{17}H_{20}N_2O_4S$ (MH^+) 349.1222, found 349.1227

3.12. Di-*tert*-butyl-4-(2-oxo-1,2-dihydrobenzo[*cd*]indole-6-sulfonamido)butyl phosphate (35)

Tetrazole (3 wt % solution in CH_3CN, 0.4 mL, 0.16 mmol) and di-*tert*-butyl-*N,N*-diisopropylphosphoramidite (95%, 0.24 mL, 0.12 mmol) were added to a solution of **32** (0.25 mg, 0.078 mmol) in THF (3 mL) and the reaction mixture was stirred at room temperature under argon for 16 h. The mixture was cooled to 0 °C and H_2O_2 (70% aqueous, 0.1 mL) was added. After 15 min, the cooling bath was removed and the mixture was stirred for a further 6 h, and then aqueous Na_2SO_3 (10%, 2 mL) was added with water bath cooling. After 25 min, the organic solvents were evaporated and the aqueous residue was extracted with EtOAc (3 × 10 mL). The extracts were washed with brine, dried with Na_2SO_4, and evaporated. The resulting residue was purified by silica gel column chromatography, eluting with 90:10 EtOH–hexane, to yield pure compound **35** (24 mg, 60%) as a yellow residue. ^{1}H NMR (300 MHz, MeOH-d_4) δ 8.72 (d, J = 8.4 Hz, 1H), 8.11 (d, J = 7.6 Hz, 1H), 8.09 (d, J = 7.0 Hz, 1H), 7.90 (dd, J = 7.1, 8.3 Hz, 1H), 7.04 (d, J = 7.6 Hz, 1H), 3.79 (dd, J = 5.9, 12.0 Hz, 2H), 2.89 (t, J = 6.3 Hz, 2H), 1.55–1.40 (22H); ^{13}C NMR (75 MHz, MeOH-d_4) δ 171.4, 143.9, 133.8, 131.5, 131.1, 130.6, 128.3, 128.0, 126.2, 106.0, 84.1, 84.0, 67.7, 43.2, 30.1, 30.08, 28.3, 26.9; EIMS m/z (rel intensity) 1024 ($2MH^+$, 45), 513 (MH^+, 100), 457 (8); negative ion EIMS m/z (rel intensity) 556 ($M-HCOO^-$, 38], 511 [$(M-H^+)^-$, 100]; HRMS m/z calcd for $C_{23}H_{33}N_2O_7PS$ 513.1824 (MH^+), found 513.1822.

3.13. Di-*tert*-butyl-5-(2-oxo-1,2-dihydrobenzo[*cd*]indole-6-sulfonamido)pentyl phosphate (36)

Tetrazole (3 wt % solution in CH_3CN, 3.0 mL, 1.3 mmol) and di-*tert*-butyl-*N,N*-diisopropylphosphoramidite (95%, 0.26 mL, 0.75 mmol) were added to a solution of **33** (180 mg, 0.54 mmol) in THF (5 mL) and the reaction mixture was stirred at room temperature under argon for 16 h. The mixture was cooled to 0 °C and H_2O_2 (70% aqueous, 1.5 mL) was added. After 15 min, the cooling bath was removed and the mixture was stirred for a further 6 h, and then aqueous Na_2SO_3 (10%, 5 mL) was added with water bath cooling. After 25 min, the organic solvents were evaporated and the aqueous residue was extracted with EtOAc (3 × 10 mL). The extracts were washed with brine, dried with Na_2SO_4, and evaporated. The resulting yellow residue was purified on a silica gel column made with EtOAc–hexane (7:3), eluting with EtOAc–hexane (9:1), to result in pure compound **36** (125 mg, 44%). ^{1}H NMR (300 MHz, acetone-d_6) δ 10.22 (s, 1H), 8.66 (d, J = 8.1 Hz, 1H), 8.04 (d, J = 7.5 Hz, 1H), 7.98 (d, J = 6.9 Hz, 1H), 7.82 (t, J = 6.9 Hz, 1H), 7.01 (d, J = 7.6 Hz, 1H), 6.78 (t, J = 4.8 Hz, 1H), 3.73 (dd, J = 5.1, 6.3 Hz, 2H), 2.82 (q, J = 5.7 Hz, 2H), 1.36 (m, 22H), 1.22 (m, 2H); ^{13}C NMR (75 MHz, acetone-d_6) δ 206.1, 169.1, 143.2, 133.0, 130.7, 129.7, 127.6, 127.3, 125.51, 125.0, 104.858, 82.0, 66.8, 66.7, 43.1. 29.6, 22.9; ESIMS m/z (rel intensity) 549 (MNa^+, 100); negative ion ESIMS m/z (rel intensity) 531 (92), 525 ($[M-H^+]^-$, 100); HRMS m/z calcd for $C_{24}H_{35}N_2O_7PS$ (MNa^+) 549.1800, found 549.1802.

3.14. Di-*tert*-butyl-5-(2-oxo-1,2-dihydrobenzo[*cd*]indole-6-sulfonamido)hexyl phosphate (37)

Tetrazole (3 wt % solution in CH_3CN, 2.1 mL, 1.0 mmol) and di-*tert*-butyl-*N,N*-diisopropyl-phosphoramidite (95%, 0.20 mL, 0.8 mmol) were added to a solution of **34** (172 mg, 0.5 mmol) in THF (5 mL) and the reaction mixture was stirred at room temperature under argon for 16 h. The mixture was cooled to 0 °C and H_2O_2 (70% aqueous, 1.2 mL) was added. After 15 min, the cooling bath was removed and the mixture was stirred for a further 6 h, and then aqueous Na_2SO_3 (10%, 5 mL) was added with water bath cooling. After 25 min, the organic solvents were evaporated and the aqueous residue was extracted with EtOAc (3 × 10 mL). The extracts were washed with brine, dried with Na_2SO_4, and evaporated. The resulting yellow residue was purified by silica gel column chromatography, eluting with EtOAc–hexane (8:1), to result in pure compound **37** (95 mg, 18%) as a yellow oil. ^{1}H NMR (300 MHz, $CDCl_3$) δ 9.91 (s, 1H), 8.66 (d, J = 8.4 Hz, 1H), 8.06 (d, J = 7.6 Hz, 1H), 7.98 (d, J = 7.0 Hz, 1H), 7.73 (t, J = 7.3 Hz, 1H), 6.99 (d, J = 7.6 Hz, 1H), 6.90 (s, 1H), 3.84 (q, J = 6.5 Hz, 2H), 2.87 (q, J = 4.2 Hz, 2H), 1.47 (m, 22H), 1.16 (m, 4H); ^{13}C NMR (75 MHz, $CDCl_3$) δ 169.8, 142.9, 142.2, 132.5, 130.3, 129.7, 128.6, 126.6, 125.1, 124.8, 105.1, 82.9, 82.8, 66.9, 66.8, 42.7. 29.6, 29.3, 25.8, 24.8; ESIMS m/z (rel intensity) 541 (M^+, 9), 429 (100); negative ion ESIMS m/z (rel intensity) 539 ($[M-H^+]^-$, 3), 483 ($[M-t\mathrm{Bu}^+]^-$, 100); HRMS m/z calcd for $C_{25}H_{37}N_2O_7PS$ (MH^+) 541.2137, found 541.2136.

3.15. 4-(2-Oxo-1,2-dihydrobenzo[*cd*]indole-6-sulfonamido)-butyl dihydrogen phosphate (38)

TFA (0.03 mL, 0.35 mmol) was added to a solution of **35** (18 mg, 0.035 mmol) in CH_2Cl_2 (2 mL) and the solution was stirred at room temperature for 16 h. The mixture was evaporated, and the residue was washed with CH_2Cl_2 (3 × 10 mL) and dried under vacuum to yield compound **38** (35 mg, 69%) as a light-yellow solid: mp 194–196 °C. ^{1}H NMR (300 MHz, MeOH-d_4) δ 8.72 (d, J = 8.1 Hz, 1H), 8.12 (d, J = 6.3 Hz, 1H), 8.09 (d, J = 5.4 Hz, 1H), 7.90 (dd, J = 7.2, 8.4 Hz, 1H), 7.05 (d, J = 7.5 Hz, 1H), 3.83 (dd, J = 6.0, 12.3 Hz, 2H), 2.88 (t, J = 6.6 Hz, 2H), 1.56 (t, J = 6.3 Hz, 2H), 1.52 (t, J = 5.1 Hz, 2H); ^{13}C NMR (75 MHz, MeOH-d_4) δ 171.5, 143.9, 133.8, 131.5, 130.6, 128.3, 128.0, 126.2, 106.0, 67.0, 43.3, 28.5, 26.9; EIMS m/z (rel intensity) 801 ($2MH^+$, 55), 401 (MH^+, 100), 303 (19); negative ion EIMS m/z (rel intensity) 799 [$(2M-H^+)^-$, 100], 399 [$(M-H^+)^-$, 21]; HRMS m/z calcd for $C_{15}H_{17}N_2O_7PS$ (MH^+) 401.0572, found 401.0580. Anal. Calcd for $C_{15}H_{17}N_2O_7PS{\cdot}1H_2O$: C, 43.06; H, 4.58; N, 6.70. Found: C, 43.35; H, 4.25; N, 6.56.

3.16. 5-(2-Oxo-1,2-dihydrobenzo[*cd*]indole-6-sulfonamido)-pentyl dihydrogen phosphate (39)

TFA (0.1 mL, 1.27 mmol) was added to a solution of **36** (120 mg, 0.23 mmol) in CH_2Cl_2 (3 mL) and the solution was allowed to stir at room temperature for 16 h overnight. The mixture was evaporated, and the residue was washed with CH_2Cl_2 (3 × 10 mL) and dried to provide compound **39** (65 mg, 62%): mp 209–212 °C. ^{1}H NMR (300 MHz, MeOH-d_4) δ 8.71 (d, J = 8.4 Hz, 1H), 8.11 (d, J = 7.5 Hz, 1H), 8.09 (d, J = 6.9 Hz, 1H), 7.91 (t, J = 7.3 Hz, 1H), 7.04 (d, J = 7.6 Hz, 1H), 3.73 (q, J = 6.6 Hz, 2H), 2.82 (t, J = 6.6 Hz, 2H), 1.40 (m, 6H); ^{13}C NMR (75 MHz, MeOH-d_4) δ 171.5, 143.9, 133.8, 131.5, 131.1, 130.6, 128.3, 128.0, 126.2, 106.0, 67.4, 43.6, 30.9, 30.8, 30.1, 23.6; ESIMS m/z (rel intensity) 829, ($[2M+H]^+$, 7), 415 (MH^+, 100), 317 (10); negative ion ESIMS m/z (rel intensity) 827 ($[2M-H^+]^-$, 100), 413 ($[M-H^+]^-$, 19); HRMS m/z calcd for $C_{16}H_{19}N_2O_7PS$ (MH^+) 415.0729, found 415.0725. Anal. Calcd for $C_{16}H_{19}N_2O_7PS$: C, 46.38; H, 4.62; N, 6.67; S, 7.74. Found: C, 45.99; H, 4.67; N, 6.63; S, 7.78.

3.17. 5-(2-Oxo-1,2-dihydrobenzo[*cd*]indole-6-sulfonamido)hexyl dihydrogen phosphate (40)

TFA (0.12 mL, 1.7 mmol) was added to a solution of **37** (90 mg, 0.17 mmol) in CH_2Cl_2 (5 mL) and the solution was allowed to stir at room temperature for 16 h overnight. The mixture was evaporated, and the residue was washed with CH_2Cl_2 (3 × 10 mL) and dried to give compound **40** (22 mg, 31%): mp 224–228 °C. ^{1}H NMR (300 MHz, MeOH-d_4) δ 8.73 (d, J = 8.4 Hz, 1H), 8.12 (d, J = 7.6 Hz, 1H), 8.11 (d, J = 6.9 Hz, 1H), 7.91 (dd, J = 7.2, 8.3 Hz, 1H), 7.05 (d, J = 7.6 Hz, 1H), 3.83 (q, J = 6.6 Hz, 2H), 2.82 (t, J = 6.9 Hz, 2H), 1.45 (m, 2H), 1.35 (m, 2H), 1.18 (m, 4H); ^{13}C NMR (75 MHz, MeOH-d_4) δ 171.5, 143.9, 133.8, 131.5, 131.2, 130.8, 128.3, 128.1, 126.3, 106.0, 67.6, 67.5, 43.7, 31.3, 31.2, 30.4, 27.1, 26.0; ESIMS m/z (rel intensity) 451, (MNa^+, 10), 429 (MH^+, 100); HRMS m/z calcd for $C_{17}H_{21}N_2O_7PS$ (MH^+) 429.0885, found 429.0890. Anal. Calcd for $C_{17}H_{21}N_2O_7PS$: C, 47.66; H, 4.94; N, 6.54; S, 7.45. Found: C, 47.31; H, 4.70; N, 6.47; S, 7.45.

3.18. Diethyl 4-iodobutylphosphonate (46)

Sodium hydride (60%) in mineral oil (0.75 g, 18.8 mmol) was suspended in anhydrous THF (70 mL) and the reaction mixture cooled to −20 °C. A solution of diethyl phosphate (2.0 g, 14.5 mmol) in THF (10 mL) was introduced under argon. After stirring at −20 °C for 1 h, 1,4-diiodobutane (**43**) (3.8 mL, 29.0 mol) was added and the mixture was stirred at −10 °C for 18 h. The mixture was then concentrated under vacuum, taken up in EtOAc (30 mL) and water (30 mL), and the pH adjusted to 8 with concentrated HCl. The EtOAc was washed with brine, dried over Na_2SO_4, and evaporated to a colorless oil, which was purified by silica gel flash column chromatography with CH_2C1_2–EtOAc (3:7) as eluant to afford **46** (2.6 g, 57%) as a colorless oil. ^{1}H NMR (300 MHz, $CDCl_3$) δ 4.09–4.01 (m, 4H), 3.20 (t, J = 6.6 Hz, 2H), 1.86 (m, 2H), 1.70 (m, 4H), 1.27 (t, J = 7.0 Hz, 6H); ^{13}C NMR (75 MHz, $CDCl_3$) δ 61.5, 61.41, 33.8, 33.6, 25.4, 23.5, 23.4, 16.4, 16.4, 5.5; EIMS m/z (rel intensity) 321 (MH^+, 15), 343 (MNa^+, 100); HRMS m/z calcd for $C_8H_{18}IO_3P$ (MNa^+) 342.9936, found 342.9944.

3.19. Diethyl 4-iodopentylphosphonate (47)

Sodium hydride (60%) in mineral oil (0.75 g, 18.8 mmol) was suspended in anhydrous THF (70 mL) and the reaction mixture cooled to −20 °C. A solution of diethyl phosphate (2.0 g, 14.5 mmol) in THF (10 mL) was introduced under argon. After stirring at −20 °C for 1 h, 1,5-diiodopantane (**44**) (2.6 mL, 17.4 mol) was added and the mixture was stirred at −10 °C for 18 h. The mixture was then concentrated in vacuo, taken up in EtOAc (30 mL) and water (30 mL), and the pH adjusted to 8 with concentrated HCl. The EtOAc was washed with brine, dried over Na_2SO_4, and evaporated to a colorless oil, which was purified by flash silica gel column chromatography using CH_2C1_2 as eluant to yield **47** (2.5 g, 52%) as a colorless oil. ^{1}H NMR (300 MHz, $CDCl_3$) δ 3.78–3.70 (m, 4H), 2.84 (t, J = 6.9 Hz, 2H), 1.53–1.20 (m, 6H), 1.16 (m, 2H), 0.96 (t, J = 7.0 Hz, 6H); ^{13}C NMR (75 MHz, $CDCl_3$) δ 60.8, 60.7, 32.3, 30.8, 30.5, 25.8, 23.9, 20.9, 20.8, 15.9, 15.86, 5.9; EIMS m/z (rel intensity) 335 (MH^+, 100), 207 (14); HRMS m/z calcd for $C_9H_{20}IO_3P$ (MH^+) 335.0273, found 335.0283.

3.20. Diethyl 4-(1,3-dioxoisoindolin-2-yl)butylphosphonate (48)

A DMF solution (5 mL) of iodobutylphosphonate **46** (1.0 g, 3.13 mmol) and of potassium phthalimide (1.16 g, 6.26 mmol) was stirred at 100 °C for 8 h. The mixture was cooled to 25 °C and the precipitated material filtered off. The filtrate was concentrated in vacuo and the residue taken up in water (50 mL). After extraction with diethyl ether (3 × 30 mL), the organic phase was dried (Na_2SO_4) and evaporated, and the residue purified by flash silica gel column chromatography using CH_2C1_2–EtOAc (1:9) as eluant to afford **48** (0.9 g, 85%) as white solid: mp 52–54 °C. ^{1}H NMR (300 MHz, $CDCl_3$) δ 7.75 (m, 4H), 4.13–4.02 (m, 4H), 3.64 (t, J = 6.7 Hz, 2H), 1.91–1.72 (m, 4H), 1.63–1.57 (m, 2H), 1.34 (t, J = 7.0 Hz, 6H); ^{13}C NMR (75 MHz, $CDCl_3$) δ 169.4, 135.2, 133.0, 123.9, 62.94, 62.86, 37.9, 30.1, 29.9, 26.1, 24.2, 20.7, 20.6, 16.8, 16.7; EIMS m/z (rel intensity) 340 (MH^+, 2), 362 (MNa^+, 100); HRMS m/z calcd for $C_{16}H_{22}NO_5P$ (MNa^+) 362.1133, found 362.1139.

3.21. Diethyl 4-(1,3-dioxoisoindolin-2-yl)pentylphosphonate (49)

A DMF (5 mL) solution of iodopentylphosphonate **47** (1.0 g, 3.0 mmol) and potassium phthalimide (1.11 g, 6.0 mmol) was stirred at 100 °C for 8 h. The mixture was cooled to 25 °C and the precipitated material filtered off. The filtrate was concentrated in vacuo and the residue taken up in water (50 mL). After extraction with diethyl ether (3 × 30 mL), the organic phase was dried (Na_2SO_4), evaporated and the residue purified by flash silica gel column chromatography using silica gel and CH_2C1_2–EtOAc (1:9) as eluant to afford **49** (0.91 g, 86%) as yellowish semisolid. ^{1}H NMR (300 MHz, MeOH-d_4) δ 7.76 (m, 4H), 4.09–4.03 (m, 4H), 3.62 (t, J = 7.0 Hz, 2H), 1.85–1.60 (m, 6H), 1.42 (m, 2H), 1.30 (t, J = 7.0 Hz, 6H); ^{13}C NMR (75 MHz, MeOH-d_4) δ 169.6, 135.2, 133.2, 124.0, 63.04, 62.95, 38.4, 28.9, 28.6, 28.4, 26.5, 24.6, 23.0, 22.9, 16.8, 16.7; EIMS m/z (rel intensity) 354 (MH^+, 87), 376 (MNa^+, 100); HRMS m/z calcd for $C_{17}H_{24}NO_5P$ (MNa^+) 376.1290, found 376.1296.

3.22. Diethyl 4-(2-oxo-1,2-dihydrobenzo[*cd*]indole-6-sulfonamido)butylphosphonate (52)

Compound **48** (0.4 g, 1.3 mmol) was dissolved in absolute ethanol (8 mL) and 98% hydrazine hydrate (0.18 mL, 3.9 mmol) was added. The reaction mixture was stirred at reflux for 3 h. The ethanol was removed in vacuo and the residue purified by flash column chromatography with silica gel, eluting with 5% MeOH in ethyl acetate, to afford compound **50** (0.2 g, 81%) as a colorless oil. Amine **50** (117 mg, 0.56 mmol) and derivative **15** (100 mg, 0.37 mmol) were dissolved in THF (5 mL). The reaction mixture was stirred at room temperature for 12 h. The THF was removed in vacuo and the residue purified by flash silica gel column chromatography, eluting with 1% MeOH in ethyl acetate, to afford compound **52** (0.1 g, 61%) as yellow oil. ^{1}H NMR (300 MHz, MeOH-d_4) δ 8.68 (d, J = 8.3 Hz, 1H), 8.08 (d, J = 7.6 Hz, 1H), 8.04 (d, J = 7.2 Hz, 1H), 7.93 (dd, J = 7.2, 8.3 Hz, 1H), 7.02 (d, J = 7.5 Hz, 1H), 3.98 (m, 4H), 2.86 (m, 2H), 1.61 (m, 2H), 1.46 (m, 4H), 1.24 (t, J = 7.1 Hz, 6H); ^{13}C NMR (75 MHz, MeOH-d_4) δ 171.3, 143.8, 133.9, 133.7, 131.5, 131.0, 130.5, 128.2, 127.9, 126.1, 106.0, 63.1, 63.0, 43.1, 31.1, 30.9, 26.0, 24.1, 20.4, 20.3, 16.73, 16.65; EIMS m/z (rel intensity) 441 (MH^+, 100), 463 (MNa^+, 69); negative ion EIMS m/z (rel intensity) 439 [$(M-H^+)^-$, 100]; HRMS m/z calcd for $C_{19}H_{25}N_2O_6PS$ (MH^+) 441.1249, found 441.1251.

3.23. Diethyl 4-(2-oxo-1,2-dihydrobenzo[*cd*]indole-6-sulfonamido)pentylphosphonate (53)

Compound **49** (0.25 g, 0.7 mmol) was dissolved in absolute ethanol (5 mL) and 98% hydrazine hydrate (0.1 mL, 2.1 mmol) was added. The reaction mixture was stirred at reflux for 3 h. The ethanol was removed in vacuo and the residue purified by silica gel flash column chromatography, eluting with 5% MeOH in ethyl acetate, to afford compound **51** (0.13 g, 82%) as a colorless oil. Amine

51 (125 mg, 0.56 mmol) and derivative **15** (100 mg, 0.37 mmol) were dissolved in THF (5 mL). The reaction mixture was stirred at room temperature for 12 h. The THF was removed in vacuo and the residue purified by silica gel flash column chromatography with silica gel, eluting with 1% MeOH in ethyl acetate, to afford compound **53** (110 mg, 67%) as a yellow oil. ^{1}H NMR (300 MHz, MeOH-d_4) δ 8.67 (d, J = 8.4 Hz, 1H), 8.07 (d, J = 7.6 Hz, 1H), 8.04 (d, J = 7.0 Hz, 1H), 7.86 (dd, J = 7.0, 8.4 Hz, 1H), 7.01 (d, J = 7.6 Hz, 1H), 4.01 (m, 4H), 2.84 (t, J = 6.5 Hz, 2H), 1.49 (m, 2H), 1.46 (m, 6H), 1.25 (t, J = 7.1 Hz, 6H); ^{13}C NMR (75 MHz, MeOH-d_4) δ 171.3, 143.8, 133.9, 133.7, 131.4, 131.1, 130.6, 128.2, 127.9, 126.5, 126.1, 106.0, 63.1, 63.0, 43.4, 29.8, 28.3, 28.1, 26.3, 24.5, 22.7, 22.6, 16.74; EIMS m/z (rel intensity) 455 (MH^+, 100), 477 (MNa^+, 44); negative ion EIMS m/z (rel intensity) 453 [$(M-H^+)^-$, 100]; HRMS m/z calcd for $C_{20}H_{27}N_2O_6PS$ (MH^+) 455.1406, found 455.1411.

3.24. 4-(2-Oxo-1,2-dihydrobenzo[*cd*]indole-6-sulfonamido)-butylphosphonic acid (54)

Bromotrimethylsilane (0.6 mL, 0.45 mmol) was added to a solution of compound **52** (50 mg, 0.12 mmol) in CH_2Cl_2 (4 mL). After stirring for 36 h at 25 °C, the volatiles were removed in vacuo, and the residue was purified by passing it through lipophilic Sephadex (LH20), using CH_2Cl_2–MeOH (8:2) as eluant, to produce **54** (28 mg, 64%) as a yellowish solid: mp 259–261 °C (dec). ^{1}H NMR (300 MHz, DMSO-d_6) δ 11.13 (s, 1H), 8.65 (d, J = 8.1 Hz, 1H), 8.09 (d, J = 6.9 Hz, 1H), 8.00 (d, J = 7.5 Hz, 1H), 7.93 (dd, J = 7.2, 8.1 Hz, 1H), 7.78 (t, J = 7.2 Hz, 1H), 7.04 (d, J = 7.5 Hz, 1H), 2.70 (m, 2H), 1.39 (m, 6H); ^{13}C NMR (125 MHz, MeOH-d_4 and DMSO-d_6) δ 169.4, 135.2, 133.0, 123.9, 62.94, 62.86, 37.9, 30.1, 29.9, 26.1, 24.2, 20.7, 20.6, 16.8, 16.7; EIMS m/z (rel intensity) 791 ($2MNa^+$, 100), 384 (MNa^+, 27), 179 (38); negative ion EIMS m/z (rel intensity) 767 [$(2M-H^+)^-$, 100], 383 [$(M-H^+)^-$, 75]; HRMS m/z calcd for $C_{15}H_{17}N_2O_6PS$ (MNa^+) 407.0443, found 407.0441. Anal. Calcd for $C_{15}H_{17}N_2O_6PS{\cdot}CH_2Cl_2$: C, 40.95; H, 4.08; N, 5.97. Found: C, 41.18; H, 4.16, N, 6.30.

3.25. 4-(2-Oxo-1,2-dihydrobenzo[*cd*]indole-6-sulfonamido)-pentylphosphonic acid (55)

Bromotrimethylsilane (0.6 mL, 0.44 mmol) was added to the solution of compound **53** (50 mg, 0.11 mmol) in CH_2Cl_2 (4 mL). After stirring for 36 h at 25 °C, the volatiles were removed in vacuo, and the residue was purified by lipophilic Sephadex column (LH20), using CH_2Cl_2–MeOH (8:2) as eluant, to result in **55** (34 mg, 61%) as a yellowish solid: mp 294–296 °C (dec). ^{1}H NMR (500 MHz, DMSO-d_6) δ 11.13 (s, 1H), 8.66 (d, J = 8.3 Hz, 1H), 8.09 (d, J = 6.9 Hz, 1H), 8.01 (d, J = 7.5 Hz, 1H), 7.94 (dd, J = 7.2, 8.1 Hz, 1H), 7.76 (t, J = 7.2 Hz, 1H), 7.05 (d, J = 7.5 Hz, 1H), 2.72 (m, 2H), 1.30 (m, 6H), 1.18 (m, 2H); ^{13}C NMR (125 MHz, DMSO-d_6) δ 169.0, 142.6, 132.5, 130.4, 129.8, 128.9, 127.0, 126.2, 125.0, 124.5, 104.9, 42.2, 28.7, 27.9, 27.2, 27.0, 26.9, 22.4; negative ion EIMS m/z (rel intensity) 795 [$(2M-H^+)^-$, 100], 398 [$(M-H^+)^-$, 55]. Anal. Calcd for $C_{16}H_{19}N_2O_6PS{\cdot}H_2O$: C, 46.15; H, 5.08; N, 6.73. Found: C, 46.22; H, 4.93, N, 6.8.

3.26. Diethyl 1,1-difluoro-4-iodobutylphosphonate (61)

A solution of LDA (2.9 mL, 5.85 mmol, 2M solution) in dry THF (10 mL) was added at −78 °C to a solution of diethyl (difluoromethyl)phosphonate (**57**) (1.0 g, 5.32 mmol) in HMPA (2 mL). After stirring for 1 h at −78 °C, a solution of diiodopropane (**58**) (1.35 mL, 11.69 mmol) in THF (10 mL) was added and the mixture was allowed to stir for 6 h at −78 °C. The reaction mixture was then poured into ether (50 mL)-20% H_3PO_4 (10 mL) and the aqueous layer was extracted with ether (20 mL × 2). The combined ether extracts were washed with brine, dried over Na_2SO_4, and concentrated under vacuum. The residual oil was purified by silica gel column chromatography using CH_2Cl_2-30% EtOAc as eluent to give **61** (0.35 g, 19%) as a yellow oil: ^{1}H NMR (300 MHz, $CDC1_3$) δ 4.23 (dt, J = 7.2, 14.9 Hz, 4H), 3.18 (t, J = 6.6 Hz, 2H), 2.09 (m, 4H), 1.34 (t, J = 6.9 Hz, 6H); ^{13}C NMR (75 MHz, $CDCl_3$) δ 121.5 (dt), 64.4, 64.3, 34.6 (m), 24.8, 24.8, 16.3, 16.2, 4.9; EIMS m/z (rel intensity) 357 (MH^+, 100), 379 (MNa^+, 78); HRMS m/z calcd for $C_8H_{16}F_2IO_3P$ (MH^+) 356.9928, found 356.9927.

3.27. Diethyl 1,1-difluoro-5-iodopentylphosphonate (62)

A solution of LDA (2.5 mL, 4.97 mmol, 2M solution) in dry THF (10 mL) was added at −78 °C to a solution of diethyl (difluoromethyl)phosphonate (**57**) (0.85 g, 4.52 mmol) in HMPA (2 mL). After stirring for 1 h at −78 °C, a solution of diiodobutane (**59**) (1.3 mL, 9.94 mmol) in THF (10 mL) was added and the mixture was allowed to stir for 6 h at −78 °C. The reaction mixture was then poured into ether (50 mL)-20% H_3PO_4 (10 mL) and the aqueous layer was extracted with ether (20 mL × 2). The combined ether extracts were washed with brine, dried over Na_2SO_4, and concentrated under vacuum. The residual oil was purified by silica gel column chromatography using CH_2Cl_2-30% EtOAc as eluent to give **62** (0.28 g, 17%) as a yellow oil: ^{1}H NMR (300 MHz, $CDC1_3$) δ 4.22 (dt, J = 7.2, 14.9 Hz, 4H), 3.13 (t, J = 6.8 Hz, 2H), 2.03 (m, 2H), 1.80 (m, 2H), 1.66 (m, 2H), 1.34 (t, J = 7.0 Hz, 6H); ^{13}C NMR (75 MHz, $CDCl_3$) δ 112.3 (dt), 63.8, 63.7, 32.2 (m), 21.3, 21.2, 15.8, 15.7, 5.2; EIMS m/z (rel intensity) 371 (MH^+, 100), 343 (29); HRMS m/z calcd for $C_9H_{18}F_2IO_3P$ (MH^+) 371.0085, found 371.0082.

3.28. Diethyl 1,1-difluoro-5-iodohexylphosphonate (63)

A solution of LDA (2.5 mL, 4.97 mmol, 2M solution) in dry THF (10 mL) was added at −78 °C to a solution of diethyl (difluoromethyl)phosphonate (**57**) (0.85 g, 4.52 mmol) in HMPA (2 mL). After stirring for 1 h at −78 °C, a solution of diiodopentane (**60**) (1.3 mL, 9.94 mmol) in THF (10 mL) was added and the mixture was allowed to stir for 6 h at −78 °C. The reaction mixture was then poured into ether (50 mL)-20% H_3PO_4 (10 mL) and the aqueous layer was extracted with ether (20 mL × 2). The combined ether extracts were washed with brine, dried over Na_2SO_4, and concentrated under vacuum. The residual oil was purified by silica gel column chromatography using CH_2Cl_2-30% EtOAc as eluent to give **63** (0.4 g, 23%) as a yellow oil: ^{1}H NMR (300 MHz, $CDC1_3$) δ 4.13 (dt, J = 7.1, 15.0 Hz, 4H), 3.06 (t, J = 6.9 Hz, 2H), 1.90 (m, 2H), 1.7.2 (m, 2H), 1.49 (m, 2H), 1.34 (m, 2H), 1.24 (t, J = 7.0 Hz, 6H); ^{13}C NMR (75 MHz, $CDCl_3$) δ 119.0 (dt), 64.1, 64.0, 33.5 (m), 32.8, 29.8, 19.4, 19.3, 16.2, 16.1, 6.2; EIMS m/z (rel intensity) 385 (MH^+, 55), 329($MH^+-C_4H_8$, 100); HRMS m/z calcd for $C_{10}H_{20}F_2IO_3P$ (MH^+) 385.0241, found 385.0243.

3.29. 2-Oxo-1,2-dihydrobenzo[*cd*]indole-6-sulfonamide (67)

Compound **15** (300 mg, 1.12 mmol) was dissolved in dry THF (10 mL). Ammonia gas was dissolved in the reaction mixture at −78 °C for 20 min. The reaction mixture was stirred at room temperature for 6 h. The yellow precipitate was filtered and dried to give compound **67** (0.22 g, 79%) as yellow solid: mp 272–275 °C (dec). ^{1}H NMR (300 MHz, DMSO-d_6) δ 8.62 (d, J = 8.3 Hz, 1H), 8.09 (d, J = 7.0 Hz, 1H), 8.03 (d, J = 7.5 Hz, 1H), 7.92 (dd, J = 7.3 Hz, 8.0 Hz, 1H), 7.05 (d, J = 7.5 Hz, 1H); ^{13}C NMR (75 MHz, DMSO-d_6) δ 169.4, 142.2, 132.8, 130.7, 130.09, 130.08, 127.1, 126.3, 125.2, 124.5, 105.1; EIMS m/z (rel intensity) 531 [$(2M^++Cl^-)$, 60], 496 ($2M^+$, 100), 283 [(M^++Cl^-), 33], 248 (M^+, 85). Anal. Calcd for

$C_{11}H_8N_2O_3S$: C, 53.22; H, 3.25; N, 11.28. Found: C, 53.24; H, 3.33, N, 11.42.

3.30. Diethyl 1,1-difluoro-4-(2-oxo-1,2-dihydrobenzo[*cd*]indole-6-sulfonamido)butyl-phosphonate (68)

K_2CO_3 (83 mg, 0.6 mmol) was added to the solution of iodo derivative **61** (79 mg, 0.22 mmol) and amine derivative **67** (50 mg, 0.20 mmol) in DMF (3 mL). The reaction mixture was stirred at room temperature for 12 h. Water (25 mL) was added to the reaction mixture and the mixture was extracted with diethyl ether (20 mL × 3). The combined organic extracts were washed with brine, dried (Na_2SO_4), and evaporated. The residue was purified by flash silica gel column chromatography, eluting with EtOAc–petroleum ether (7:3), to afford compound **68** (60 mg, 63%) as a yellow oil. ^{1}H NMR (300 MHz, acetone-d_6) δ 8.73 (d, J = 8.4 Hz, 1H), 8.18 (d, J = 7.5 Hz, 1H), 8.10 (d, J = 7.0 Hz, 1H), 7.94 (t, J = 8.1 Hz, 1H), 7.28 (d, J = 7.5 Hz, 1H), 6.80 (s, 2H), 4.24–4.14 (m, 4H), 4.07 (t, J = 6.7 Hz, 2H), 2.24–2.09 (m, 4H), 1.27 (t, J = 7.0 Hz, 6H); ^{13}C NMR (75 MHz, acetone-d_6) δ 168.2, 144.1, 134.0, 131.5, 131.0, 130.8, 127.3, 126.5, 125.6, 120.6, 104.4, 64.9, 64.8, 40.1, 32.0 (m), 21.2, 16.6, 16.5; EIMS m/z (rel intensity) 499 (MNa^+, 100), 477 (MH^+, 23), 444 (29); HRMS m/z calcd for $C_{19}H_{23}F_2N_2O_6PS$ (MNa^+) 499.0880, found 499.0889.

3.31. Diethyl 1,1-difluoro-4-(2-oxo-1,2-dihydrobenzo[*cd*]-indole-6-sulfonamido)pentyl-phosphonate (69)

K_2CO_3 (83 mg, 0.6 mmol) was added to a solution of iodo derivative **62** (82 mg, 0.22 mmol) and amine derivative **67** (50 mg, 0.20 mmol) in DMF (3 mL). The reaction mixture was stirred at room temperature for 12 h. Water (25 mL) was added to the reaction mixture and the mixture was extracted with diethyl ether (20 mL × 3). The combined organic extracts were washed with brine, dried (Na_2SO_4), and evaporated. The residue was purified by flash silica gel column chromatography, eluting with EtOAc–petroleum ether (7:3), to afford compound **69** (65 mg, 66%) as a yellow oil. ^{1}H NMR (300 MHz, acetone-d_6) δ 8.87 (d, J = 8.4 Hz, 1H), 8.31 (d, J = 7.6 Hz, 1H), 8.23 (d, J = 7.0 Hz, 1H), 8.07 (t, J = 8.1 Hz, 1H), 7.38 (d, J = 7.3 Hz, 1H), 6.94 (s, 2H), 4.38–4.28 (m, 4H), 4.15 (t, J = 6.8 Hz, 2H), 2.29–2.18 (m, 4H), 1.83 (m, 2H), 1.43 (t, J = 7.0 Hz, 6H); ^{13}C NMR (75 MHz, acetone-d_6) δ 168.2, 144.2, 133.8, 131.5, 130.9, 130.7, 127.3, 126.4, 125.5, 125.4, 120.6 (dt), 104.4, 64.8, 64.7, 40.3, 34.2 (m), 19.02, 18.91, 16.7, 16.6; EIMS m/z (rel intensity) 491 (MH^+, 100), 471 (10); negative ion EIMS m/z (rel intensity) 489 [$(M-H^+)^-$, 100], 457 (34); HRMS m/z calcd for $C_{20}H_{25}F_2N_2O_6PS$ (MH^+) 491.1217, found 491.1216.

3.32. Diethyl 1,1-difluoro-4-(2-oxo-1,2-dihydrobenzo[*cd*]indole-6-sulfonamido)-hexyl-phosphonate (70)

K_2CO_3 (83 mg, 0.6 mmol) was added to the solution of iodo derivative **63** (84 mg, 0.22 mmol) and amine derivative **67** (50 mg, 0.20 mmol) in DMF (3 mL). The reaction mixture was stirred at room temperature for 12 h. Water (25 mL) was added to the reaction mixture and the mixture was extracted with diethyl ether (20 mL × 3). The combined organic extracts were washed with brine, dried (Na_2SO_4), and evaporated. The residue was purified by flash silica gel column chromatography, eluting with EtOAc–petroleum ether (7:3), to afford compound **70** (60 mg, 59%) as a yellow oil. ^{1}H NMR (300 MHz, acetone-d_6) δ 8.71 (d, J = 8.4 Hz, 1H), 8.16 (d, J = 7.5 Hz, 1H), 8.06 (d, J = 6.9 Hz, 1H), 7.90 (t, J = 8.2 Hz, 1H), 7.20 (d, J = 7.7 Hz, 1H), 6.78 (s, 2H), 4.21 (m, 4H), 3.96 (t, J = 6.8 Hz, 2H), 2.03 (m, 2H), 1.86 (m, 2H), 1.60 (m, 2H), 1.48 (m, 2H), 1.30 (t, J = 7.0 Hz, 6H); ^{13}C NMR (75 MHz, acetone-d_6) δ 168.1, 144.2, 133.7, 131.5, 130.9, 130.6, 127.3, 126.3, 125.4, 125.3, 120.4 (dt), 104.3, 64.8, 64.7, 40.5, 34.3 (m), 27.1, 21.2, 21.1, 16.7, 16.6; EIMS m/z (rel intensity) 505 (MH^+, 100), 447 (45); HRMS m/z calcd for $C_{21}H_{27}F_2N_2O_6PS$ (MH^+) 505.1374, found 505.1375

3.33. 1,1-Difluoro-4-(2-oxo-1,2-dihydrobenzo[*cd*]indole-6-sulfonamido)butylphosphonic acid (71)

Bromotrimethylsilane (0.6 mL, 0.42 mmol) was added to the solution of compound **68** (50 mg, 0.10 mmol) in CH_2Cl_2 (4 mL). After stirring for 36 h at 25 °C, the volatiles were removed in vacuo, and the residue was purified by passing it through lipophilic Sephadex (LH20) using CH_2Cl_2–MeOH (8:2) as eluant to give **71** (32 mg, 73%) as a yellowish solid: mp 127–130 °C. ^{1}H NMR (500 MHz, MeOH-d_4) δ 8.66 (d, J = 8.1 Hz, 1H), 8.15 (d, J = 7.5 Hz, 1H), 8.00 (d, J = 6.6 Hz, 1H), 7.84 (t, J = 7.5 Hz, 1H), 7.11 (d, J = 7.5 Hz, 1H), 3.98 (t, J = 6.6 Hz, 2H), 2.15 (m, 2H), 2.07 (m, 2H); ^{13}C NMR (125 MHz, MeOH-d_4) δ 169.7, 144.0, 134.3, 131.7, 131.3, 127.2, 126.6, 126.2, 125.7, 124.9, 122.2 (dt), 105.3, 40.8, 32.4 (m), 21.6; EIMS m/z (rel intensity) 841 ($2MH^+$, 63), 421 (MH^+, 100); negative ion ESIMS m/z (rel intensity) 839 ([$2M-H^+$]$^-$, 100), 419 ([$M-H^+$]$^-$, 33); HRMS m/z calcd for $C_{15}H_{15}F_2N_2O_6PS$ (MH^+) 421.0435, found 421.0431. Anal. Calcd for $C_{15}H_{15}F_2N_2O_6PS{\cdot}H_2O$: C, 41.10; H, 3.91; N, 6.39; P, 7.07. Found: C, 41.32; H, 4.09; N, 6.58; P, 6.97.

3.34. 1,1-Difluoro-4-(2-oxo-1,2-dihydrobenzo[*cd*]indole-6-sulfonamido)pentylphosphonic acid (72)

Bromotrimethylsilane (0.6 mL, 0.42 mmol) was added to the solution of compound **69** (50 mg, 0.10 mmol) in CH_2Cl_2 (4 mL). After stirring for 36 h at 25 °C, the volatiles were removed in vacuo, and the residue was purified by passing it through lipophilic Sephadex (LH20) using CH_2Cl_2–MeOH (8:2) as eluant to give **72** (27 mg, 61%) as a yellowish solid: mp 170–173 °C. ^{1}H NMR (500 MHz, MeOH-d_4) δ 8.70 (d, J = 8.1 Hz, 1H), 8.17 (d, J = 7.5 Hz, 1H), 8.07 (d, J = 6.6 Hz, 1H), 7.87 (t, J = 7.5 Hz, 1H), 7.14 (d, J = 7.5 Hz, 1H), 3.97 (t, J = 6.6 Hz, 2H), 2.12 (m, 2H), 1.86 (m, 2H), 1.68 (m, 2H); ^{13}C NMR (125 MHz, MeOH-d_4) δ 169.7, 144.3, 134.4, 131.8, 131.3, 127.4, 126.8, 126.2, 121.0 (dt), 105.4, 40.9, 34.5 (m), 29.4, 19.6; EIMS m/z (rel intensity) 869 ($2MH^+$, 100), 435 (MH^+, 74); negative ion ESIMS m/z (rel intensity) 867 ([$2M-H^+$]$^-$, 100), 433 ([$M-H^+$]$^-$, 25); HRMS m/z calcd for $C_{16}H_{17}F_2N_2O_6PS$ (MH^+) 435.0591, found 435.0593. Anal. Calcd for $C_{16}H_{17}F_2N_2O_6PS$: C, 44.24; H, 3.94; N, 6.45; P, 7.13. Found: C, 44.39; H, 4.25; N, 6.62; P, 6.92.

3.35. 1,1-Difluoro-4-(2-oxo-1,2-dihydrobenzo[*cd*]indole-6-sulfonamido)hexylphosphonic acid (73)

Bromotrimethylsilane (0.5 mL, 0.42 mmol) was added to the solution of compound **70** (50 mg, 0.10 mmol) in CH_2Cl_2 (4 mL). After stirring for 36 h at 25 °C, the volatiles were removed in vacuo, and the residue was purified by passing it through lipophilic Sephadex (LH20) using CH_2Cl_2–MeOH (8:2) as eluant to give **73** (30 mg, 68%) as a yellowish solid: mp 90–93 °C. ^{1}H NMR (300 MHz, MeOH-d_4) δ 8.65 (d, J = 8.1 Hz, 1H), 8.13 (d, J = 7.5 Hz, 1H), 8.00 (d, J = 6.6 Hz, 1H), 7.83 (t, J = 7.5 Hz, 1H), 7.07 (d, J = 7.5 Hz, 1H), 3.90 (t, J = 6.6 Hz, 2H), 2.02 (m, 2H), 1.84 (m, 2H), 1.78 (m, 2H), 1.42 (m, 2H); ^{13}C NMR (125 MHz, MeOH-d_4) δ 169.7, 144.2, 134.3, 131.7, 131.23, 131.18, 127.3, 126.1, 125.7, 122.5 (dt), 105.3, 41.0, 34.8 (m), 29.3, 27.7, 21.7; EIMS m/z (rel intensity) 897 ($2MH^+$, 100), 449 (MH^+, 86); negative ion ESIMS m/z (rel intensity) 895 ([$2M-H^+$]$^-$, 100), 447 ([$M-H^+$]$^-$, 12); HRMS m/z calcd for $C_{17}H_{19}F_2N_2O_6PS$ (MH^+) 449.0748, found 449.0758.

Anal. Calcd for $C_{17}H_{19}F_2N_2O_6PS{\cdot}H_2O$: C, 43.78; H, 4.54; N, 6.01; P, 6.64. Found: C, 43.72; H, 4.69; N, 5.78; P, 6.41.

3.36. Ethyl 2-(2,4-bis(benzyloxy)-6-chloropyrimidin-5-ylamino)-2-oxoacetate (76)

Triethylamine (0.3 mL, 2.2 mmol) was added to a solution of compound **75** (80 mg, 0.23 mmol) in THF (5 mL). The solution was cooled to 0 °C and ethyl 2-chloro-2-oxoacetate (31 μL, 0.28 mmol) was added dropwise. The reaction mixture was stirred at 0 °C for 12 h. The solvent was distilled off under reduced pressure and the residue was dissolved in dichloromethane (20 mL) and washed with water (2 × 15 mL). The organic layer was dried and solvent was distilled off. The residue was flash column chromatographed with silica gel, eluting with 35% ethyl acetate in hexane, to afford compound **76** (78 mg, 76%) as a white semisolid. ^{1}H NMR (300 MHz, $CDCl_3$) δ 8.35 (s, 1H), 7.44–7.30 (m, 10H), 5.41 (s, 2H), 5.36 (s, 2H), 4.37 (q, J = 7.13, 2H), 1.37 (t, J = 7.14, 3H); ^{13}C NMR (75 MHz, $CDCl_3$) δ 166.4, 161.7, 159.7, 158.3, 154.5, 135.4, 135.0, 128.42, 128.37, 128.23, 128.18, 128.1, 127.8, 108.7, 70.1, 69.7, 63.6, 13.8; HRMS m/z calcd for $C_{22}H_{20}ClN_3O_5$ (MNa^+) 464.0989, found 464.0991. Anal. Calcd for $C_{22}H_{20}ClN_3O_5$: C, 59.80; H, 4.56; N, 9.51. Found: C, 59.83; H, 4.31; N, 9.80.

3.37. Ethyl 2-(6-chloro-2,4,dioxo-1,2,3,4-tetrahydropyrimidin-5-ylamino)-2-oxoethanoate (77)

Lindlar catalyst (5 mg) was added to a solution of compound **76** (50 mg, 0.113 mmol) in anhydrous ethanol (4 mL). 1,4-Cyclohexediene (90 μL, 1.13 mmol) was added and argon was bubbled through the reaction mixture for 10 min. The mixture was stirred at room temperature for 12 h. The reaction mixture was filtered through Celite, which was then washed with ethanol (2 × 5 mL). The solution was concentrated and the residue was washed several times with CH_2Cl_2 and THF. Finally, compound **77** was precipitated out by dissolving it in MeOH and adding excess diethyl ether to furnish pure compound **77** (20 mg, 68%) as a white amorphous solid: mp 174–176 °C. ^{1}H NMR (300 MHz, MeOH-d_4) δ 4.37 (q, J = 6.9 Hz, 2H), 1.37 (t, J = 6.9 Hz, 3H); ^{13}C NMR (75 MHz, MeOH-d_4) δ 162.8, 160.8, 158.8, 149.6, 129,6, 107.9, 64.2, 14.2; negative ion EIMS m/z (rel intensity) 260 [$(M-H^+)^-$, 100], 224 (43); HRMS m/z calcd for $C_8H_8ClN_3O_5$ (MNa^+) 284.0050, found 284.0053. Anal. Calcd for $C_8H_8ClN_3O_5{\cdot}0.65H_2O$: C, 35.15; H, 3.43; N, 15.37. Found: C, 34.8; H, 3.18; N, 15.10.

3.38. *N*-(6-Chloro-2,4-dioxo-1,2,3,4-tetrahydropyrimidin-5-yl)propionamide (78)

Triethylamine (0.3 mL, 2.2 mmol) was added to a solution of compound **75** (80 mg, 0.23 mmol) in THF (5 mL). The solution was cooled to 0 °C and propionyl chloride (25 μL, 0.28 mmol) was added dropwise. The reaction mixture was stirred at 0 °C for 12 h. The solvent was distilled off under reduced pressure and the residue was dissolved in dichloromethane (20 mL) and washed with water (2 × 15 mL). The organic layer was dried and solvent was distilled off. The residue was flash column chromatographed with silica gel, eluting with 35% ethyl acetate in hexane, to afford compound **78** (65 mg, 70%) as white solid: mp 122–124 °C. ^{1}H NMR (300 MHz, $CDCl_3$) δ 7.42–7.32 (m, 10H), 5.35 (s, 2H), 5.33 (s, 2H), 2.33 (q, J = 7.23, 2H), 1.37 (t, J = 7.1, 3H); ^{13}C NMR (75 MHz, $CDCl_3$) δ 172.8, 166.9, 161.2, 158.7, 135.5, 135.3, 128.4, 128.2, 127.7, 110.5, 70.0, 69.5, 29.3, 9.7; HRMS m/z calcd for $C_{21}H_{20}ClN_3O_3$ (MNa^+) 420.1091, found 420.1088. Anal. Calcd for $C_{21}H_{20}ClN_3O_3$: C, 63.40; H, 5.07; N, 10.56. Found: C, 63.66; H, 4.82; N, 10.78.

3.39. *N*-(6-Chloro-2,4-dioxo-1,2,3,4-tetrahydropyrimidin-5-yl)propanamide (79)

Lindlar catalyst (5 mg) was added to a solution of compound **78** (50 mg, 0.13 mmol) in anhydrous ethanol (4 mL). 1,4-Cyclohexediene (0.1 mL, 1.3 mmol) was added and argon was bubbled through the reaction mixture for 10 min. The mixture was stirred at room temperature for 12 h. The reaction mixture was filtered through Celite, which was then washed with ethanol (2 × 5 mL). The solution was concentrated and the residue was washed several times with CH_2Cl_2 and THF. Finally, compound **79** was precipitated out by dissolving it in MeOH and adding excess diethyl ether to furnish pure compound **79** (18 mg, 66%) as a white amorphous solid: mp 208–211 °C (dec). ^{1}H NMR (300 MHz, MeOH-d_4) δ 2.38 (q, J = 7.6 Hz, 2H), 1.18 (t, J = 7.6 Hz, 3H); ^{13}C NMR (75 MHz, MeOH-d_4) δ 177.1, 163.1, 152.0, 147.2, 109.8, 29.8, 10.1; EIMS m/z (rel intensity) 262 ($M-H^+$+2Na^+, 82), 240 (MNa^+, 100), 130 (35); negative ion EIMS m/z (rel intensity) 216 [$(M-H^+)^-$, 100], 180 (25); HRMS m/z calcd for $C_7H_8ClN_3O_3$ (MNa^+) 240.0152, found 240.0153. Anal. Calcd for $C_7H_8ClN_3O_3{\cdot}1.4H_2O$: C, 34.62; H, 4.48; N, 17.30. Found: C, 34.80; H, 4.18; N, 17.10.

3.40. Computational methods

3.40.1. Screening the database

The ZINC database maintained by the Shoichet group at UCSF is a pre-filtered comprehensive database of available compounds.[39] The ligands in this database have multiple protonation and tautomeric states. Approximately 1.03 million compounds were downloaded in SDF format with multiple tautomeric and protonation states (pH range 5.75–8.25) selected from following vendors: Asinex, Chembridge, Maybridge, Nanosyn and Sigma–Aldrich. The *M. tuberculosis* lumazine synthase crystal structure in complex with inhibitor 3-(1,3,7-trihydro-9-D-ribityl-2,6,8-purinetrione-7-yl) propane 1-phosphate (PDB: 1w19) was prepared using Protein Preparation tools in Maestro 7.5 (Schrödinger LLC, Portland, Oregon) removing all crystal water molecules. The compounds were first docked with Glide 4.0 (Schrödinger LLC, Portland, Oregon) High Throughput Virtual Screening mode without any constraints. The top 5% of hits were then screened using Glide Standard Precision (SP), applying the following pharmacophore constraints: 3 backbone hydrogen bonds to Ile83, Val81, Ala59 and the phosphate interaction to Arg128. At least 3 of these constraints had to be satisfied. For all hits with Glide Score –5 or better, log S and log P were calculated with QikProp 2.5 (Schrödinger LLC, Portland, Oregon). Compounds that were predicted with reasonable solubility (log P < 2.5 and log S > −3.6) were selected resulting in 6742 compounds. These selected compounds were docked again with Glide Extra Precision (XP). Glide XP not only offers a more extensive conformational search but also recognizes multiple protein–ligand motifs such as enclosure of lipophilic ligand substructures by hydrophobic protein residues and various hydrogen bonds in hydrophobic environments. In addition, the scoring function has additional penalty terms including desolvation of polar groups and solvent exposure of hydrophobic ligand group designed to remove potential false positives.[46] The backbone hydrogen bond constraints were again applied. The final 44 compounds that had Glide Score of −10 or better were inspected visually and 12 of them were tested based on the chemical scaffolds and interaction with the receptor for inhibition properties by enzymatic assay and Isothermal Titration Calorimetry (ITC). The visual inspection is a common practice which is important to avoid testing false positives due to assumptions and shortcomings in docking methods and scoring functions.[68] The score cutoff of −10 was chosen based on docking of several known active compounds[41] under the same condition.

3.40.2. Molecular modeling

Using Sybyl (Tripos, Inc., version 7.1), the crystal structure of the complex of compound **11** was clipped to include information within a 12 Å sphere of one of the 5 equivalent ligand molecules. Docking of the lead and synthesized compounds in the active site of *M. tuberculosis* lumazine synthase was performed with GOLD (BST, version 3.0, 2005). The programs were set to conduct 10,000 repeats for each ligand under identical conditions. The best fit result from GOLD docking was added to the complex, MMFF94 charges were loaded, and the energy of the complex was minimized using the Powell method to a termination gradient of 0.05 kcal/mol employing the MMFF94s force field, which was used to minimize steric clashes between the GOLD-docked compounds and the protein.

3.41. Isothermal titration calorimetry

Calorimetric measurements for binding analysis were carried out by using a VP-ITC MicroCalorimeter (MicroCal, Inc., Northampton, MA, USA). The reference cell was filled with water and the instrument was calibrated using standard electrical pulses. Binding isotherms were measured by direct titration. A solution of *M. tuberculosis* lumazine synthase (0.05 mM) in 100 mM potassium phosphate buffer at pH 7.1 in a total volume of 1.451 mL was titrated at 30 °C with 35 identical 8 μL injections at 3 min intervals. The syringe was filled with 5 mM compound dissolved in the same buffer. The heat evolved after each injection was obtained from the integral of the calorimetric signal. All data were evaluated with the Microcal Origin50 Software package (Microcal Software, INC., Northampton, MA, USA) supplied with the calorimeter. The heat of dilution was subtracted from the observed heat in the binding experiments. The association constants, K_a, binding enthalpy, ΔH, and stoichiometry, n, were obtained by fitting the data to standard equations for the binding using a model for one set of independent and identical binding sites as implemented in the MicroCal Origin50 package. The binding entropy ΔS and free energy ΔG of the binding were calculated from the basic thermodynamic equations, $\Delta G = -RT\ln K$ and the Gibbs–Helmholtz equation $\Delta G = \Delta H - T\Delta S$.

3.42. Enzymes used in kinetic assays

Recombinant lumazine synthase and riboflavin synthase of *M. tuberculosis* were prepared as described earlier.[43,69] The purified enzymes had specific activity of 1.2 μmol mg^{-1} h^{-1} (lumazine synthase) and 2.6 μmol mg^{-1} h^{-1} (riboflavin synthase).

3.43. Kinetic assay of lumazine synthase inhibitors

Assay mixtures contained 100 mM Tris hydrochloride, pH 7.0, 100 mM NaCl, 2% (v/v) DMSO, 5 mM dithiothreitol, 100 μM **2**, 2 μM lumazine synthase, variable concentrations of **1** (3–100 μM) and inhibitor (0–200 μM) in a volume of 0.2 mL. Assay mixtures were prepared as follows. A solution (170 μL) containing 105 mM NaCl, 5.3 mM dithiothreitol, 118 μM **2**, 2.4 μM lumazine synthase in 105 mM Tris hydrochloride, pH 7.0, was added to 4 μL of inhibitor in 100% (v/v) DMSO in a well of a 96-well microtiter plate. The reaction was started by adding 20 μL of a solution containing 105 mM NaCl, 5.3 mM dithiothreitol, and substrate **1** (30–1000 μM) in 105 mM Tris hydrochloride, pH 7.0. The formation of 6,7-dimethyl-8-D-ribityllumazine (**3**) was measured online for a period of 30 min at 27 °C with a computer-controlled plate reader at 408 nm ($\varepsilon_{Lumazine}$ = 10,200 M^{-1} cm^{-1}).

3.44. Kinetic assay of riboflavin synthase inhibitors

Assay mixtures contained 100 mM Tris hydrochloride, pH 7.0, 100 mM NaCl, 2% (v/v) DMSO, 5 mM dithiothreitol, 1 μM riboflavin synthase, variable concentrations of **3** (3–60 μM) and inhibitor (0–200 μM) in a volume of 0.2 mL. Assay mixtures were prepared as follows. A solution (170 μL) containing 105 mM NaCl, 5.3 mM dithiothreitol, 1.2 μM riboflavin synthase in 105 mM Tris hydrochloride, pH 7.0, was added to 4 μL of inhibitor in 100% (v/v) DMSO in a well of a 96-well microtiter plate. The reaction was started by adding 20 μL of a solution containing 105 mM NaCl, 5.3 mM dithiothreitol, and substrate **3** (30–600 μM) in 105 mM Tris hydrochloride, pH 7.0. The formation of riboflavin (**4**) was measured online for a period of 30 min at 27 °C with a computer-controlled plate reader at 470 nm ($\varepsilon_{Riboflavin}$ = 9600 M^{-1} cm^{-1}).

3.45. Evaluation of kinetic data

The velocity-substrate data were fitted for all inhibitor concentrations with a non-linear regression method using the program DYNAFIT.[69] Different inhibition models were considered for the calculation. K_i and K_{is} values ± standard deviations were obtained from the fit under consideration of the most likely inhibition model.

Acknowledgment

This research was made possible by NIH Grant Nos. RO1 GM51469 and R21 NS053634, the Hans Fischer Gesellschaft, and the Swedish Research Council.

Supplementary data

Supplementary data (^1H and ^{13}C NMR spectra of compounds **20**, **21**, **24**, **25**, **26**, **27**, **31**, **32**, **33**, **34**, **35**, **36**, **37**, **38**, **39**, **40**, **46**, **47**, **48**, **49**, **52**, **53**, **54**, **55**, **61**, **62**, **63**, **67**, **68**, **69**, **70**, **71**, **72**, **73**, **76**, **77**, **78** and **79**) associated with this article can be found, in the online version, at doi:10.1016/j.bmc.2010.03.072.

References and notes

1. Wang, A. *I Chuan Hsueh Pao* **1992**, *19*, 362.
2. Oltmanns, O.; Lingens, F. *Z. Naturforsch.* **1967**, *22 b*, 751.
3. Logvinenko, E. M.; Shavlovsky, G. M. *Mikrobiologiya* **1967**, *41*, 978.
4. Neuberger, G.; Bacher, A. *Biochem. Biophys. Res. Commun.* **1985**, *127*, 175.
5. Richter, G.; Ritz, H.; Katzenmeier, G.; Volk, R.; Kohnle, A.; Lottspeich, F.; Allendorf, D.; Bacher, A. *J. Bacteriol.* **1993**, *175*, 4045.
6. Ritz, H.; Schramek, N.; Bracher, A.; Herz, S.; Eisenreich, W.; Richter, G.; Bacher, A. *J. Biol. Chem.* **2001**, *276*, 22273.
7. Kaiser, J.; Schramek, N.; Eberhardt, S.; Püttmer, S.; Schuster, M.; Bacher, A. *Eur. J. Biochem.* **2002**, *269*, 5264.
8. Richter, G.; Fischer, M.; Krieger, C.; Eberhardt, S.; Lüttgen, H.; Gerstenschläger, I.; Bacher, A. *J. Bacteriol.* **1997**, *179*, 2022.
9. Bacher, A.; Richter, G.; Ritz, H.; Eberhardt, S.; Fischer, M.; Krieger, C. *Methods Enzymol.* **1997**, *280*, 382.
10. *Chemistry and Biochemistry of Flavoenzymes*; Muller, F., Ed.; CRC Press: Boca Raton, FL, 1992; Vol. 3,.
11. Richter, G.; Volk, R.; Krieger, C.; Lahm, H. W.; Röthlisberger, U.; Bacher, A. *J. Bacteriol.* **1992**, *174*, 4050.
12. Richter, G.; Krieger, C.; Volk, R.; Kis, K.; Ritz, H.; Götze, E.; Bacher, A. *Methods Enzymol.* **1997**, *280*, 374.
13. Fischer, M.; Römisch, W.; Schiffmann, S.; Kelly, M.; Oschkinat, H.; Steinbacher, S.; Huber, R.; Eisenreich, W.; Richter, G.; Bacher, A. *J. Biol. Chem.* **2002**, *277*, 41410.
14. Steinbacher, S.; Schiffmann, S.; Richter, G.; Huber, R.; Bacher, A.; Fischer, M. *J. Biol. Chem.* **2003**, *278*, 42256.
15. Fischer, M.; Haase, I.; Kis, K.; Meining, W.; Ladenstein, R.; Cushman, M.; Schramek, N.; Huber, R.; Bacher, A. *J. Mol. Biol.* **2003**, *326*, 783.
16. Fischer, M.; Haase, I.; Feicht, R.; Richter, G.; Gerhardt, S.; Changeux, J. P.; Huber, R.; Bacher, A. *Eur. J. Biochem.* **2002**, *269*, 519.
17. Bacher, A.; Eberhardt, S.; Fischer, M.; Mörtl, S.; Kis, K.; Kugelbrey, K.; Scheuring, J.; Schott, K. *Methods Enzymol.* **1997**, *280*, 389.
18. Haase, I.; Mörtl, S.; Köhler, P.; Bacher, A.; Fischer, M. *Eur. J. Biochem.* **2003**, *270*, 1025.
19. Haase, I.; Fischer, M.; Bacher, A.; Schramek, N. *J. Biol. Chem.* **2003**, *278*, 37909.
20. Schramek, N.; Haase, I.; Fischer, M.; Bacher, A. *J. Am. Chem. Soc.* **2003**, *125*, 4460.
21. Zhang, X.; Meining, W.; Fischer, M.; Bacher, A.; Ladenstein, R. *J. Mol. Biol.* **2001**, *306*, 1099.

22. Zhang, X.; Meining, W.; Cushman, M.; Haase, I.; Fischer, M.; Bacher, A.; Ladenstein, R. *J. Mol. Biol.* **2003**, *328*, 167.
23. Scheuring, J.; Kugelbrey, K.; Weinkauf, S.; Cushman, M.; Bacher, A.; Fischer, M. *J. Org. Chem.* **2001**, *66*, 3811.
24. Mörtl, S.; Fischer, M.; Richter, G.; Tack, J.; Weinkauf, S.; Bacher, A. *J. Biol. Chem.* **1996**, *271*, 33201.
25. Meining, W.; Mörtl, S.; Fischer, M.; Cushman, M.; Bacher, A.; Ladenstein, R. *J. Mol. Biol.* **2000**, *299*, 181.
26. Illarionov, B.; Eisenreich, W.; Bacher, A. *Proc. Natl. Acad. Sci. U.S.A.* **2001**, *98*, 7224.
27. Illarionov, B.; Kemter, K.; Eberhardt, S.; Richter, G.; Cushman, M.; Bacher, A. *J. Biol. Chem.* **2001**, *276*, 11524.
28. Eberhardt, S.; Richter, G.; Gimbel, W.; Werner, T.; Bacher, A. *Eur. J. Biochem.* **1996**, *242*, 712.
29. Gerhardt, S.; Schott, A. K.; Kairies, N.; Cushman, M.; Illarionov, B.; Eisenreich, W.; Bacher, A.; Huber, R.; Steinbacher, S.; Fischer, M. *Structure (Camb)* **2002**, *10*, 1371.
30. Illarionov, B.; Haase, I.; Bacher, A.; Fischer, M.; Schramek, N. *J. Biol. Chem.* **2003**, *278*, 47700.
31. Volk, R.; Bacher, A. *J. Am. Chem. Soc.* **1988**, *110*, 3651.
32. Lyne, P. D. *Drug Discovery Today* **2002**, *7*, 1047.
33. Garg, A.; Tewari, R.; Raghava, G. P. S. *BMC Bioinform.* **2010**, *11*, S53.
34. Okimoto, N.; Futatsugi, N.; Fuji, H.; Suenaga, A.; Morimoto, G.; Yanai, R.; Ohno, Y.; Narumi, T.; Taiji, M. *PLoS Comput. Biol.* **2009**, *5*, e1000528.
35. Chen, I. J.; Neamati, N.; Nicklaus, M. C.; Orr, A.; Anderson, L.; Barchi, J. J.; Kelly, J. A.; Pommier, Y.; MacKerell, A. D. *Bioorg. Med. Chem.* **2000**, *8*, 2385.
36. Hopkins, S. C.; Vale, R. D.; Kuntz, I. D. *Biochemistry* **2000**, *39*, 2805.
37. Kis, K.; Volk, R.; Bacher, A. *Biochemistry* **1995**, *34*, 2883.
38. Zhang, X.; Meining, W.; Cushman, M.; Haase, I.; Fischer, M.; Bacher, A.; Ladenstein, R. *J. Mol. Biol.* **2003**, *328*, 167.
39. Irwin, J. J.; Shoichet, B. K. *J. Chem. Inf. Model.* **2005**, *45*, 177.
40. Talukdar, A.; Breen, M.; Bacher, A.; Illarionov, B.; Fischer, M.; Georg, G.; Ye, Q.-Z.; Cushman, M. *J. Org. Chem.* **2009**, *74*, 5123.
41. Cushman, M.; Sambaiah, T.; Jin, G.; Illarionov, B.; Fischer, M.; Bacher, A. *J. Org. Chem.* **2004**, *69*, 601.
42. Morgunova, E.; Illarionov, B.; Sambaiah, T.; Haase, I.; Bacher, A.; Cushman, M.; Fischer, M.; Ladenstein, R. *FEBS J.* **2006**, *273*, 4790.
43. Morgunova, E.; Meining, W.; Cushman, M.; Illarionov, B.; Haase, I.; Jin, G.; Bacher, A.; Cushman, M.; Fischer, M.; Ladenstein, R. *Biochemistry* **2005**, *44*, 2746.
44. Morgunova, E.; Saller, S.; Haase, I.; Cushman, M.; Bacher, A.; Fischer, M.; Ladenstein, R. *J. Biol. Chem.* **2007**, *282*, 17231.
45. Cushman, M.; Yang, D.; Mihalic, J. T.; Chen, J.; Gerhardt, S.; Huber, R.; Fischer, M.; Kis, K.; Bacher, A. *J. Org. Chem.* **2002**, *67*, 6871.
46. Friesner, R. A.; Murphy, R. B.; Repasky, M. P.; Frye, L. L.; Greenwood, J. R.; Halgren, T. A.; Sanschagrin, P. C.; Mainz, D. T. *J. Med. Chem.* **2006**, *49*, 6177.
47. Guan, H.; Laird, A. D.; Blake, R. A.; Tanga, C.; Liang, C. *Bioorg. Med. Chem. Lett.* **2004**, *14*, 187.
48. Nurminen, E. J.; Mattinen, J. K.; Lonnberg, H. *J. Chem. Soc., Perkin Trans.* **1998**, *2*, 1621.
49. Heasley, H. H.; Jarosz, R.; Lynch, K. R.; Macdonald, T. L. *Bioorg. Med. Chem. Lett.* **2004**, *14*, 2735.
50. Kuzmic, P. *Anal. Biochem.* **1996**, *237*, 260.
51. Gerhardt, S.; Haase, I.; Steinbacher, S.; Kaiser, J. T.; Cushman, M.; Bacher, A.; Huber, R.; Fischer, M. *J. Mol. Biol.* **2002**, *318*, 1317.
52. Klinke, S.; Zylberman, V.; Vega, D. R.; Guimaraes, B. G.; Braden, B. C.; Goldbaum, F. A. *J. Mol. Biol.* **2005**, *353*, 124.
53. Ladenstein, R.; Schneider, M.; Huber, R.; Bartunik, H. D.; Wilson, K.; Schott, K.; Bacher, A. *J. Mol. Biol.* **1998**, *203*, 1045.
54. Zhang, Y.; Illarionov, B.; Morgunova, E.; Jin, G.; Bacher, A.; Fischer, M.; Ladenstein, R.; Cushman, M. *J. Org. Chem.* **2008**, *73*, 2715.
55. Ritsert, K.; Huber, R.; Turk, D.; Ladenstein, R.; Schmidt-Bäse, K.; Bacher, A. *J. Mol. Biol.* **1995**, *253*, 151.
56. Stirtan, W. G.; Withers, S. G. *Biochemistry* **1996**, *35*, 15057.
57. Kim, C. U.; Luh, B. Y.; Misco, P. F.; Bronson, J. J.; Hitchcock, M. J. M.; Ghazzouli, I.; Martin, J. C. *J. Med. Chem.* **1990**, *33*, 1207.
58. Pevzner, L. M. *Russ. J. Gen. Chem.* **2006**, *76*, 1354.
59. Bako, P.; Novak, T.; Ludanyi, K.; Pete, B.; Toke, L.; Keglevich, G. *Tetrahedron: Asymmetry* **1999**, *10*, 2373.
60. Chun, Y. J.; Park, J. H.; Oh, G. M.; Hong, S. I.; Kim, Y. J. *Synthesis* **1994**, 909.
61. Billups, W. E.; Arney, B. E., Jr.; Lin, L.-J. *J. Org. Chem.* **1984**, *49*, 3437.
62. Burton, D. J.; Takei, R.; Shina-Ya, S. *J. Fluorine Chem.* **1981**, *18*, 197.
63. Burton, D. J.; Flynn, R. M. *J. Fluorine Chem.* **1980**, *15*, 263.
64. Burton, D. J.; Flynn, R. M. *J. Fluorine Chem.* **1977**, *10*, 329.
65. Picotin, G.; Miginiac, P. *J. Org. Chem.* **1997**, *52*, 4796.
66. Cushman, M.; Mihalic, J. T.; Kis, K.; Bacher, A. *J. Org. Chem.* **1999**, *64*, 3838.
67. Yu, T.-Y.; O'Connor, R. D.; Sivertsen, A. C.; Chiauzzi, C.; Poliks, B.; Fischer, M.; Bacher, A.; Haase, I.; Cushman, M.; Schaefer, J. *Biochemistry* **2008**, *47*, 13942.
68. Klebe, G. Chap 1 Virtual screening: Scope and limitation (p3-24). In Virtual Screening in Drug Discovery edit by Juan Alvarez and Brian Shoichet CRC Press **2005**, Boca Raton, FL.
69. Kuzmic, P. *Anal. Biochem.* **1996**, *237*, 260.